# Nonequilibrium Phase Transitions in Interacting Particle Systems

(Transições de Fase de Não-equilíbrio em Sistemas de Partículas Interagentes)

Adriana Gomes Moreira

Tese apresentada à Universidade Federal de Minas Gerais como requisito parcial para a obtenção do grau de Doutor em Ciências (Física)

Orientada pelo Professor Ronald Dickman
Co-orientada pelo Professor Jafferson Kamphorst Leal da Silva

Agosto de 1996

# Acknowledgements

*I would like to thank*

*Professor Ronald Dickman, for being such a dedicated advisor, teaching me so much and encouraging me through the hard moments, and mostly, for being my friend.*

*Professor Jafferson K. Leal da Silva, for nicely guiding my first steps into science.*

*My beloved Carlos, for supporting me throughout this journey, comforting me with nice words and a beautiful smile.*

*My beloved family, that with their unconditional love made of me a very happy human being.*

*My adorable friends, Téia, Letícia, Heliana, Fabienne and Suely for the support, nice conversations and useful advices.*

*All my friends for the affection that gave me strength to go on.*

*Professor Luiz Paulo Vaz, for all the help and patience in computer matters.*

*Iwan Jensen, for helping me so much (even not being aware of that).*

*Professors Tânia Tomé Martins de Castro (USP), Wagner Figueiredo (UFSC), Antônio Sérgio Teixeira Pires (UFMG) and João Florêncio Júnior (UFMG) for kindly accepting to take part in the committee, and for helpful suggestions.*

*The Conselho Nacional de Desenvolvimento Científico e Tecnológico (CNPq-Brazil) for financial support of this work.*

# Index

# Abstract

We study the two-dimensional contact process (CP) with quenched disorder in the form of random dilution of a fraction $x$. A qualitative picture of the phase diagram is obtained through mean-field theory (MFT). Monte Carlo simulations show that the relative shift in the critical point, $[\lambda_c(x)-\lambda_c(0)]/\lambda_c(0)$ is in reasonable agreement with MFT, for small values of $x$. As expected on the basis of the Harris criterion, the critical exponents governing the order parameter and the survival probability take values different from those of the pure model. We also study the critical spreading dynamics of the diluted model. In the pure model, spreading from a single particle at the critical point $\lambda_c(0)$ is characterized by the critical exponents of directed percolation: in $2+1$ dimensions, $\delta = 0.46$, $\eta = 0.214$, and $z = 1.13$. Disorder causes a dramatic change in the critical behavior of the contact process.

We also study the one-dimensional pair-contact process via time-dependent series expansions. Numerical results provide reasonable estimates for the location of the critical point.

# Resumo

Estudamos o processo de contato diluído (DCP) bidimensional. Desordem é introduzida na forma de diluição, com uma fração $x$ de sítios sendo removida aleatoriamente da rede. Uma descrição qualitativa do diagrama de fases é obtida através da teoria de campo médio na aproximação de blocos. Simulações de Monte Carlo mostram que o deslocamento relativo do ponto crítico, $[\lambda_c(x) - \lambda_c(0)]/\lambda_c(0)$, para $x$ pequeno, está de acordo com os resultados obtidos por campo médio. Os expoentes críticos relacionados com o parâmetro de ordem e a probabilidade de sobrevivência do modelo diluído são diferentes dos expoentes do modelo puro, como era esperado pelo critério de Harris. Usando simulações dependentes do tempo estudamos a evolução do modelo a partir de uma única semente. No modelo puro, o comportamento crítico é caracterizado por leis de potência descritas pelos expoentes críticos de percolação dirigida: em $2+1$ dimensões, $\delta = 0.46$, $\eta = 0.214$, e $z = 1.13$. A presença de desordem causa uma mudança drástica no comportamento crítico do modelo.

Estudamos também o processo de contato de pares unidimensional utilizando o método de expansão em séries dependente do tempo. Estimativas razoáveis para a localização do ponto crítico foram obtidas.

# Chapter 1

# Introduction

Statistical mechanics has been used to describe systems in equilibrium quite successfully. In these systems, statistical fluctuations are due either to thermal agitation or to impurities. In the past few decades, general theories of phase transitions and also of critical phenomena have been developed, unifying understanding of the liquid-vapor transition, magnetic transitions, liquid crystals, and other systems. Understanding of critical phenomena in *nonequilibrium* steady states, is still developing, however. Since the steady-state probability distribution in these systems is not known a priori, analysis of nonequilibrium systems must be based upon their dynamics. Some of these systems have been found to exhibit a nonequilibrium phase transition, which is marked by a boundary between an active steady state and an absorbing state. Attempts at a better understanding of nonequilibrium phase transitions have led statistical physicists to study numerous models, such as reaction-diffusion systems, driven diffusive lattice gases and Ising models with competing dynamics.

In this work we are mainly interested in the issue of universality of critical behavior, which has been a prime theoretical motivation for studying critical phenomena. In particular we investigate the effects of quenched disorder on the critical behavior of the contact process, an interacting particle system exhibiting a continuous phase transition to a unique absorbing state. A typical interacting particle system, possessing an absorbing state, consists of many particles evolving according to a Markov process governed by irreversible transition rules. We also study the pair-contact process, a model with multiple absorbing configurations, whose critical spreading dynamics presents nonuniversal behavior.

This thesis is organized as follows. Basic concepts of critical phenomena and an introduction to nonequilibrium phase transitions are presented in chapter 2. In

chapter 3 we study the two-dimensional contact process under quenched disorder via one- and two-site mean-field cluster expansions. In chapter 4 we approach the diluted contact process through Monte Carlo simulations. In chapter 5 we study the one-dimensional pair-contact process via time-dependent series expansions, focusing on the evolution of the model from a state close to the absorbing state. Concluding remarks and outlook are given in chapter 6.

# Chapter 2

# Introduction to Nonequilibrium Phase Transitions

## 2.1 Introduction

This chapter has the aim of introducing the reader to a particular class of nonequilibrium models – interacting particle systems exhibiting a continuous phase transition to an absorbing state.

We consider the following topics. In section (2.2) we review some basic concepts in critical phenomena. In section (2.3) we discuss the contact process (CP) and related models. In section (2.4) we review scaling behavior in critical phenomena. A brief introduction of the most useful methods applied to nonequilibrium models is given in section (2.5). We discuss universality in section (2.6), and in section (2.7) we give an overview on basic concepts of disordered systems.

## 2.2 Basic Concepts

The main objective of this section is to help the reader, especially one not familiar with recent developments in statistical physics, to understand and perhaps enjoy this work. For this purpose we introduce the contact process (CP) which is the simplest model of nonequilibrium phase transitions. The CP [1, 2] is an interacting particle system that can be seen as a model for the spread of an infection. In this context, each site of the lattice represents an individual that may be infected or healthy. The infection spreads through direct contact between infected and healthy individuals. The spreading of the infection depends upon an "infection parameter" ($\lambda$). Infected

individuals recover at unit rate, and are then susceptible to reinfection. Since an individual must have at least one sick neighbor to become infected, the state in which all the individuals are healthy is *absorbing*. An absorbing state is a configuration from which the system cannot escape.

The persistence of the epidemic is controlled by the infection parameter. If $\lambda$ is too small, extinction of the infection at long times is certain; on the other hand, large values of $\lambda$ assure that the infection will spread indefinitely. The boundary between persistence and extinction is marked by a *critical point*, which is denoted by $\lambda_c$. The critical parameter $\lambda_c$ separates the two possible *steady states* the system can reach at asymptotic times, namely a disease-free or absorbing state and a surviving epidemic or active state. It turns out that $\lambda_c$ marks a *continuous phase transition* between an absorbing state and an active state. In a continuous phase transition the stationary density of infected individuals ($\rho$) rises continuously from zero as the infection parameter is increased. A quantity like $\rho$ is referred to as an *order parameter*. Near the critical point the order parameter goes to zero following a power law characterized by a *critical exponent*: $\rho \sim (\lambda - \lambda_c)^\beta$ where $\beta$ is the critical exponent associated with the order parameter. The independence of the critical exponents on most system details is known as *universality*. Models with the same set of critical exponents form a *universality class*. In general a universality class is determined by global features such as dimensionality, dimension of the order parameter and range of the interactions.

Models possessing a continuous transition into a unique absorbing state generally belong to the same universality class as the directed percolation (DP), according to the DP conjecture [3, 4, 5, 6]. The presence of conservation laws can influence the critical behavior of a model. Also models with multiple absorbing configurations have presented a non-DP time-dependent behavior [39, 40, 41].

## 2.3 Contact Process and Related Models

In this section we present a few models that exemplify the main properties of nonequilibrium phase transitions. We start by defining the contact process as a model for creation and annihilation of particles on a lattice, followed by directed percolation and the Ziff-Gulari-Barshad (ZGB) surface-reaction model.

The contact process (CP) [1] is a one-component model, whose importance resides in its simplicity. The CP can be defined as follows. Each site of a hypercubic lattice is either vacant or occupied by a particle. Particles are created at vacant sites at rate $\lambda n/2d$, where $n$ is the number of occupied nearest neighbors, and are annihilated

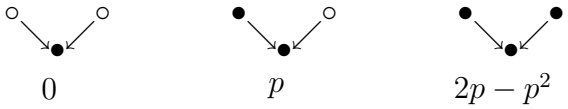


Figure 2.1: Diagram showing the rules for the directed percolation with bond probability $p$ on the square lattice.

at unit rate, independent of the surrounding configuration. The order parameter is the stationary particle density; it vanishes in the vacuum state, which is absorbing. As $\lambda$ is increased beyond $\lambda_c$, the model presents a continuous phase transition from the vacuum to an active steady state.

Directed percolation (DP) [7] can be defined as the ordinary bond percolation problem, in which bonds are randomly distributed on a lattice with concentration $p$, with the introduction of a preferential direction to the problem. Fig. (2.1) shows the transition rules for directed bond percolation. The top row of Fig. (2.2) represents the initial state, which is connected by diagonal bonds to the row below. Each of these oriented bonds is present only with probability $p$ independent of the other bonds. A site in this lattice is connected to the origin if and only if it is connected to a site in the previous layer that is connected to the origin. There is a critical concentration $p_c$, below which the probability of an infinite "percolating" cluster is zero. Near $p_c$ the system features the characteristic lengths $\xi_\perp$ and $\xi_\parallel$, perpendicular to and parallel to the main direction, respectively, that diverge like

$$\xi_\perp \sim (p_c - p)^{-\nu_\perp} \tag{2.1}$$

$$\xi_\parallel \sim (p_c - p)^{-\nu_\parallel} \tag{2.2}$$

An interesting interpretation arises if we take the biased direction as time; the remaining $(d-1)$-dimensions may represent a lattice in space [8]. The latter interpretation allows a mapping of DP onto Reggeon field theory (RFT) [9], a high energy particle physics theory, which models the scattering cross section of high energetic nuclei. Analysis of RFT shows that it has a phase transition in the same universality class as DP [10, 11]. The CP transition also belongs to the universality class of directed percolation. In fact, the $d$-dimensional contact process corresponds to directed percolation in $d+1$ dimensions. This can be seen by considering a discrete-time analog of the contact process in which all sites are updated simultaneously. A $d$-dimensional system is represented by a $(d+1)$-dimensional lattice whose layers record the configuration at times $t = 0, 1, 2, \cdots$. A site is occupied in layer $t$ only if one of its neighbors or the

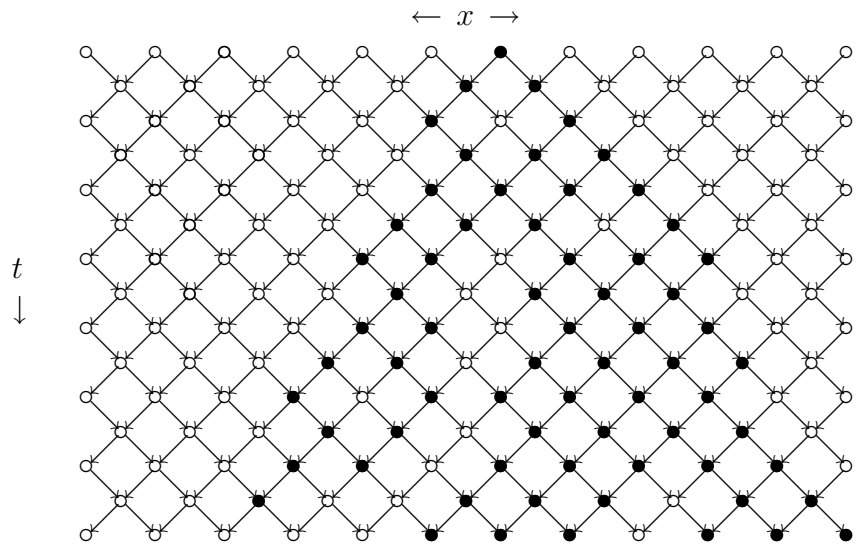


Figure 2.2: Typical time evolution from a single particle in dynamical directed percolation, particles are represented by a •, lattice sites by a ○, and the directed bonds by arrows. The cluster is typical of those observed at large values of the spreading probability $p$.

site itself were occupied in layer $t-1$ (this avoids spontaneous creation). A site can be vacant in layer $t$ even if it is occupied in layer $t-1$ (annihilation). Directed percolation is the simplest way of implementing this simultaneous updating. Thus "survival" of a trial in the CP corresponds to "percolation" in DP. Although one model cannot be mapped onto the other, the CP and DP are equivalent as far as critical behavior is concerned.

A wide variety of catalysis models have been considered in the study of nonequilibrium phase transitions. Perhaps the best known is the Ziff-Gulari-Barshad (ZGB) model for the oxidation of carbon monoxide ($CO$) on a catalytic surface [12]. Such reactions are of great technological importance. The model is defined on a square lattice, which represents the catalytic surface. The reaction proceeds via the Langmuir-Hinshelwood mechanism: both species must be chemisorbed. Adsorption of $CO$ molecules occurs at rate $y$ on a vacant site; adsorption of $O_2$ requires a nearest-neighbor pair of empty sites. Adsorbed $O$ and $CO$ react when they are sitting at nearest-neighbor sites, followed by the immediate desorption of the product, $CO_2$ [13]. If by any chance, the lattice is completely covered by one of the reactants, $CO$ or $O$, we say that the lattice is poisoned. A $CO$-poisoned lattice has all sites occupied by $CO$, which blocks $O$ adsorption and consequently inhibits the reaction. Once the system enters a poisoned state it remains in it indefinitely. Thus such a poisoned state

is absorbing. Depending on $y$, the system can exist in one of three phases: poisoned by $O$, poisoned by $CO$, or reactive. The model presents a first order phase transition from the $CO$-poisoned to the active state, and a continuous transition from the oxygen-covered state to the active state. This latter belongs in the universality class of directed percolation [3, 14, 15].

## 2.4 Scaling Behavior

The idea of scaling, which is strongly associated with continuous phase transitions, was first introduced on a phenomenological basis by Widom [16]. He conjectured that the equation of state is a homogeneous function of the relevant thermodynamic variables in the vicinity of the critical point. Near the critical point, the system is subject to strong fluctuations correlated over very large times and distances, being characterized by a divergence of the correlation length at the critical point. Based on this fact, Kadanoff [17] gave an intuitive picture for scaling. The scaling hypothesis states that the divergence of the correlation length is responsible for the singular dependence of physical quantities on the distance from the critical point. Scaling gained a firmer basis with the advent of the renormalization group devised by Wilson [18].

### 2.4.1 Steady-state Behavior

As we have already seen, a nonequilibrium phase transition occurs in the stationary regime (between the stationary absorbing state and an active stationary state). In the following we try to give an idea of the main aspects of steady-state critical behavior.

#### Critical Behavior

Near the critical point, thermodynamic response functions are dominated by a singular contribution, associated with a diverging correlation length. The singular contribution depends (in the simplest cases) on a single variable, the correlation length, and generalized homogeneity reflects how the correlation length depends on the relevant thermodynamic variables. The latter, in equilibrium, are reduced temperature and field, or reduced chemical potential in a fluid system.

Before we go on, we shall make a brief digression to discuss generalized homogeneous functions, as they are the starting point of the scaling theory. By definition,

a function $F(x)$ is *homogeneous* if it satisfies,

$$F(\lambda x) = g(\lambda)F(x) \tag{2.3}$$

for all values of the parameter $\lambda$. The function $g(\lambda)$ must always be power-like, $g(\lambda) = \lambda^p$. Analogously, for a homogeneous function of two variables we have

$$F(\lambda x, \lambda y) = \lambda^p F(x, y). \tag{2.4}$$

Generalized homogeneity involves different scaling dependencies upon two (or more) arguments, so:

$$F(\mu^u x, \mu^v y) = \mu^p F(x, y). \tag{2.5}$$

By setting $\lambda = \mu^p$ we get

$$F(\lambda^{\frac{u}{p}} x, \lambda^{\frac{v}{p}} y) = \lambda F(x, y) \tag{2.6}$$

$$F(\lambda^a x, \lambda^b y) = \lambda F(x, y) \tag{2.7}$$

where $a = u/p$ and $b = v/p$. Thus a generalized homogeneous function is characterized by two (or more) powers, here $a$ and $b$.

As critical behavior of thermodynamic variables is described by generalized homogeneous functions we expect that such quantities as the order parameter, susceptibility, etc., follow power-laws near the critical point [16]. Hence the stationary density near the critical point, ($\lambda > \lambda_c$), grows as

$$\overline{\rho}_\bullet \propto |\lambda - \lambda_c|^\beta \tag{2.8}$$

where $\beta$ is the order parameter critical exponent. As in equilibrium critical phenomena, nonequilibrium systems, undergoing a continuous phase transition, feature a characteristic length scale, the correlation length ($\xi$), near the critical point. The correlation length diverges at criticality as

$$\xi \propto |\lambda - \lambda_c|^{-\nu_\perp} \tag{2.9}$$

where $\nu_\perp$ is the correlation-length exponent. The relaxation time, $\tau$, the time it takes for a system to reach the steady state, also diverges at the critical point,

$$\tau \propto |\lambda - \lambda_c|^{-\nu_\parallel}, \tag{2.10}$$

where $\nu_\parallel$ is the relaxation-time exponent [19].

**Finite-size Scaling**

In a finite system, the correlation length cannot become infinite, since it is limited by the linear extent of the system, $L$. The singularities that characterize phase transitions and critical points only emerge in the limit $L \to \infty$; in finite systems they are rounded over a region roughly delimited by $\xi \geq L$, where $\xi$ is the correlation length in the infinite-size limit. Next we show how to use this size-dependence to locate the critical point and estimate exponents.

As we are working in a finite volume, we expect that finite-size effects become relevant near the critical point, as the infinite-size correlation length $\xi \approx L$. Thus, according to finite-size scaling hypothesis [20, 21], various quantities depend on the system size through the ratio $L/\xi$, or equivalently through the variable $\Delta L^{1/\nu_\perp}$, where $\Delta \equiv |\lambda - \lambda_c|$. For example, expressing the order parameter as a function of $\Delta$ and $L$, we have

$$\overline{\rho}_\bullet(\Delta, L) \propto L^{-\beta/\nu_\perp} f(\Delta L^{1/\nu_\perp}). \tag{2.11}$$

We must assume that $f(x) \propto x^\beta$ for $x \to \infty$ in order to recover Eq. (2.8) in the limit $L \to \infty$. At the critical point, $\Delta = 0$, we obtain

$$\overline{\rho}_\bullet(0, L) \propto L^{-\beta/\nu_\perp}. \tag{2.12}$$

Log-log plots of the stationary density *versus* the system size can be very useful in locating the critical point.

### 2.4.2 Time-dependent Behavior

We cannot talk about scaling behavior without mentioning the time-dependent analysis introduced by Grassberger and de la Torre [22]. The basic idea is to study the spread of a population starting from a configuration close to the absorbing state, in general a single seed at the origin. Of prime interest are $P(t)$, the probability that the system has not entered the absorbing state at time $t$, $n(t)$, the mean number of particles (averaged over all trials, including those that do not survive until time $t$), and $R^2(t)$, the mean-square distance of particles from the origin. In the subcritical region, $\lambda < \lambda_c$, $P(t)$ and $n(t)$ decay exponentially. In this regime, as annihilation is the dominant event the population cannot spread very far, thus we expect $R^2(t) \propto t$. In this regime the conditional probability of finding a particle at $r$ at time $t$, given

a single particle at the origin at $t = 0$, decays exponentially at long times and large distances:

$$\rho(r,t) \simeq \exp(-r/\xi)\exp(-t/\tau), \tag{2.13}$$

where $\xi$ and $\tau$ are the characteristic spatial extent and the characteristic lifetime, both diverging as $\lambda \to \lambda_c$. Thus a cluster emanating from a single seed has a characteristic lifetime $\tau$ and spatial extent $\xi$. In the supercritical regime,$(\lambda > \lambda_c)$, there is a nonzero probability that the process continues to spread from this seed as $t \to \infty$; the active region expands at a constant rate, so that $n(t) \propto t^d$ and $R^2(t) \propto t^2$. The process dies out with probability one at the critical point, but the mean lifetime diverges. In the absence of a characteristic time scale, the asymptotic evolution of these quantities follows power-laws,

$$P(t) \propto \quad t^{-\delta} \tag{2.14}$$

$$n(t) \propto \quad t^{\eta} \tag{2.15}$$

$$R^2(t) \propto \quad t^{z} \tag{2.16}$$

where $\delta, \eta$ and $z$ are critical exponents. Thus log-log plots of $P(t), n(t)$ and $R^2(t)$ approach straight lines at the critical point, and show a positive or negative curvature in the supercritical or subcritical regimes, respectively. The exponents $\delta, \eta$ and $z$ are provided by the asymptotic slopes of the critical curves. In general we have to expect finite-time corrections to scaling of the type

$$P(t) \propto t^{-\delta}(1 + at^{-\theta} + bt^{-\delta'} + \cdots). \tag{2.17}$$

Similar expressions hold for $n(t)$ and $R^2(t)$. This implies for the local slope $\delta(t)$ the behavior

$$\delta(t) = \delta + at^{-\theta} + bt^{-\delta'} + \cdots, \tag{2.18}$$

and analogous expressions for $\eta(t)$ and $z(t)$.

## 2.5 Analytical Methods

In this section we give an overview of the most widely-applied methods for nonequilibrium phase transitions in lattice models. In order to illustrate mean-field cluster expansions [23] we apply the simplest approximation, the site-approximation, to the

| process | rate | $\Delta\rho_\bullet$ |
|---|---|---|
| $\bullet\circ\bullet \to \bullet\bullet\bullet$ | $\lambda\rho_\bullet^2(1-\rho_\bullet)$ | 1 |
| $\bullet\circ\circ \to \bullet\bullet\circ$ | $\frac{\lambda}{2}\rho_\bullet(1-\rho_\bullet)^2$ | 1 |
| $\circ\circ\bullet \to \circ\bullet\bullet$ | $\frac{\lambda}{2}\rho_\bullet(1-\rho_\bullet)^2$ | 1 |
| $\bullet \to \circ$ | $\rho_\bullet$ | -1 |

Table 2.1: Rates of change for the one-dimensional contact process in site-approximation level. • represents a particle and ∘ a vacancy.

one-dimensional contact process. Then we present an example of the mean-field renormalization group which, in general, leads to better estimates of critical parameters than the ones obtained by mean-field theories. A brief summary of the basic idea of series expansions follows.

### 2.5.1 Mean-field Theory

We consider the CP as defined in section (2.3) with $d = 1$. Let $\sigma_i = 1$ represent the state of site $i$ when occupied by a particle, and $\sigma_i = 0$ when vacant. The probability that site $i$ is occupied at time $t$ is represented by $P(\sigma_i = 1; t) \equiv \rho_\bullet$. In Table 2.1 are summarized the rates of change for each process of the one-dimensional CP. In the first process creation occurs at the central site at rate $\lambda$; by treating each site independently and assuming spatial homogeneity one can write the probability for finding the cluster in this configuration as $\rho_\bullet^2(1-\rho_\bullet)$. Each contribution to the evolution equation is given by the product of the rate of change and the change in the number of particles, $\Delta\rho_\bullet$. Thus, considering the four possible events showed in Table 2.1, the equation of motion for $\rho_\bullet$ is given by

$$\frac{d\rho_\bullet}{dt} = \rho_\bullet(\lambda - 1) - \lambda\rho_\bullet^2. \tag{2.19}$$

For $\lambda \leq 1$ the only stationary solution is the vacuum, $\overline{\rho}_\bullet = 0$. For $\lambda > 1$ we also find an active stationary solution, namely $\overline{\rho}_\bullet = 1 - \lambda^{-1}$. We can see that for $\lambda > \lambda_c = 1$ the active state is stable and the vacuum unstable. $\lambda_c$ marks a critical point, at which the stationary density changes continuously but in a singular manner. Thus $\overline{\rho}_\bullet$ is the order parameter for this transition, assuming a nonzero value only for $\lambda > \lambda_c$. Near the critical point the order parameter generally follows a power law,

$$\overline{\rho}_\bullet \propto \Delta^\beta \qquad (\Delta > 0), \tag{2.20}$$

where $\Delta \equiv \lambda - \lambda_c$. Hence, in the mean-field approximation of the CP we find $\beta = 1$, as $\overline{\rho}_\bullet = \Delta + \mathcal{O}(\Delta^2)$ for $\Delta > 0$. This simple mean-field analysis predicts a qualitatively correct phase diagram, while it provides very poor values for the critical point and exponents. This is a direct consequence of neglecting any correlations among the sites; in fact they are highly correlated. It is worth remarking that the mean-field exponents are incorrect for spatial dimensions $d < d_c = 4$, where $d_c$ is the upper critical dimension, above which the critical exponents are mean-field like. In mean-field theory one assumes that all neighbors of a given site behave in the same way. Spatial homogeneity is also realized in high dimensionality. Therefore it is reasonable to expect that mean-field theory is exact in the limit of large $d$. In fact, most systems have a particular dimensionality, known as its critical dimensionality, above which mean-field theory gives the right description of critical properties.

### 2.5.2 Mean-field Renormalization Group

The mean-field renormalization group (MFRG) has been successfully employed in nonequilibrium systems [24, 25, 26]. The method can be seen as a combination of the usual mean-field and renormalization group ideas.

As an example of a MFRG analysis we apply it to the one-dimensional contact process. By considering a two-site cluster we study the evolution of the probability of finding sites $i$ and $j$ in states $\sigma_i$ and $\sigma_j$ at time $t$, $P(\sigma_i, \sigma_j; t)$. $\sigma$ can take the values $\{0, 1\}$ indicating a vacant and an occupied site, respectively. In order to simplify the notation we denote $P(1,1;t) \equiv \rho_{\bullet\bullet}$, $P(0,0;t) \equiv \rho_{\circ\circ}$, and $P(0,1;t) + P(1,0;t) \equiv \rho_{\bullet\circ}$. Thus, for a two-site cluster we get:

$$\begin{aligned}
\frac{d\rho_{\circ\circ}}{dt} &= -\lambda x \rho_{\circ\circ} + \rho_{\bullet\circ} \\
\frac{d\rho_{\bullet\circ}}{dt} &= -\frac{1}{2}\rho_{\bullet\circ}\lambda(1+x) - \rho_{\bullet\circ} + 2\rho_{\bullet\bullet} + \lambda x \rho_{\circ\circ} \\
\frac{d\rho_{\bullet\bullet}}{dt} &= -2\rho_{\bullet\bullet} + \frac{1}{2}\lambda\rho_{\bullet\circ}(1+x)
\end{aligned} \tag{2.21}$$

where $x$ is the probability of any site outside the cluster being occupied. As we are studying a continuous phase transition we may let the field $x$ become arbitrarily small in the vicinity of the critical point. Thus the order parameter $\rho_\bullet^{(2)}(\lambda, x)$ (for the 2-site cluster) can be linearized in $x$. In the steady state one obtains

$$\rho_\bullet^{(2)} \equiv \rho_{\bullet\bullet} + \frac{1}{2}\rho_{\bullet\circ} = x\left(\frac{\lambda}{2} + \frac{\lambda^2}{4}\right) + \mathcal{O}(x^2). \tag{2.22}$$

Applying the same reasoning to a one-site cluster, the evolution equation for $P(1;t) \equiv \rho_\bullet$ is simply

$$\frac{d\rho_\bullet}{dt} = -\rho_\bullet + \lambda'(1-\rho_\bullet)x', \tag{2.23}$$

where $x'$ is the probability that any other site is occupied, and $\lambda'$ is the creation parameter for the one-site cluster. Notice that if we let $\rho_\bullet = x'$ we recover the mean-field site approximation of eq. (2.19). In the steady state, and expanding in $x'$, we find $\rho_\bullet \approx \lambda' x' + \mathcal{O}(x'^2)$.

The main assumption of MFRG is that the two approximate order parameters rescale in the same manner as the two fields. Thus, on the basis of a Wilson renormalization group strategy [18], a mapping $(\lambda, x) \to (\lambda', x')$ is obtained by requiring

$$\rho_\bullet^{N'}(\lambda', x') = L^{d-y}\rho_\bullet^{N}(\lambda, x) \tag{2.24}$$

$$x' = L^{d-y}x \tag{2.25}$$

to hold to leading orders in $x$. $L$ is the length-rescaling factor associated with the two clusters $L = (N/N')^{1/d}$. The exponent $(d-y)$ is the scaling dimension of the order parameter. An estimate for the critical point, $\lambda_c$, may be found by expanding eq. (2.24) for small $x$, leading to a relation $\lambda' = f(\lambda)$, from which $\lambda_c$ may be determined by locating the fixed point(s) of this transformation. Thus, assuming that $\rho_\bullet(\lambda', x')$ and $\rho_\bullet^{(2)}(\lambda, x)$ scale like $x'$ and $x$, respectively, we find the recursion relation

$$\lambda' = \frac{\lambda}{2} + \frac{\lambda^2}{4}, \tag{2.26}$$

which has the fixed point $\lambda_c = 2$. This represents a substantial improvement over the one-site value. (Naturally, better results are achieved using even larger clusters.) For the one-dimensional CP, series expansions [27] and simulations [22] yield $\lambda_c \simeq 3.2978$. The method also provides estimates for the critical exponents. As an example we compute the correlation length exponent defined through the relation, $\xi \sim (\lambda - \lambda_c)^{-\nu_\perp}$. After a rescaling the new correlation length will be

$$\xi' \sim L^{-1}\xi, \tag{2.27}$$

which in terms of $\lambda$ and $\lambda'$ becomes

$$(\lambda' - \lambda_c) \sim L^{1/\nu_\perp}(\lambda - \lambda_c). \tag{2.28}$$

If the transformation $\lambda' = f(\lambda)$ is regular (Wilson's fundamental assumption), we may linearize it around the fixed point:

$$(\lambda' - \lambda_c) = (\lambda - \lambda_c)[\frac{\partial \lambda'}{\partial \lambda}]_{\lambda=\lambda_c} \tag{2.29}$$

which together with eq. (2.28) gives

$$[\frac{\partial \lambda'}{\partial \lambda}]_{\lambda=\lambda_c} \sim L^{1/\nu_\perp}. \tag{2.30}$$

In our example $L = (N/N') = 2$, and from the recursion relation we find that $[\partial\lambda'/\partial\lambda] = 3/2$ at $\lambda_c$. Thus

$$\nu_\perp = \frac{\ln 2}{\ln 3/2} = 1.71, \tag{2.31}$$

that should be compared to $\nu_\perp = 1.100(5)$ obtained from transfer-matrix methods [28].

### 2.5.3 Series Expansions

Series expansions have been of great importance in the study of nonequilibrium systems [14, 27, 29, 30], and are probably the most precise method available. Unfortunately, its application to the CP and related models is limited to low dimensional systems.

One is typically interested in finding the critical parameters of some function $F(z)$ that exhibits a power-law behavior in the vicinity of a critical point $z_c$, i.e.,

$$F(z) \approx A(z_c - z)^{-\alpha}. \tag{2.32}$$

If $F$ is analytic in the neighborhood of the origin it is possible to represent it through a Taylor series, $F(z) = \sum_{j=0}^{\infty} a_j z^j$. One begins a series analysis by determining as many terms as possible in this expansion. Once one has the series one needs a method for extracting the critical parameters. The method of Padé approximants [31, 32, 33, 34] provides a powerful general technique for approximating a function $F(z)$, having simple poles at $z_1, \cdots, z_n$. One assumes that the series for $F(z)$ is the expansion of a ratio

$$F(z) \sim \frac{P_N(z)}{Q_M(z)} \equiv \frac{p_0 + p_1 z + \cdots + p_N z^N}{q_0 + q_1 z + \cdots + q_M z^M} \tag{2.33}$$

of two polynomials, of order $N$ and $M$. This quotient is called the $[N, M]$ Padé approximant. The coefficients are chosen such that they agree with the first $M+N+1$

series coefficients of the expansion of $F(z)$. The usefulness of these approximants comes from the fact that a function like $F(z)$ will have a logarithmic derivative of the form $d\ln F(z)/dz$ and a simple pole at $z_c$, which is very well represented by Padé approximants. If the series is well behaved the critical point is associated with the first singularity on the positive real axis. Thus $z_c$ is given by locating the pole of the Padé approximant and the critical exponent is the corresponding residue.

## 2.6 Universality

Universality of critical behavior has been a central topic in the study of continuous phase transitions. The fact that many different models can belong to the same universality class shows the irrelevance of the microscopic characteristics and, at the same time, a strong dependence on general properties such as system dimension, dimension of the order parameter, range of the interactions, conservation laws, etc. One of the most important achievements in nonequilibrium phase transitions is that a wide variety of models exhibiting a continuous transition into a unique absorbing state have been shown to belong to the same universality class as directed percolation [13, 3, 4, 5].

So far we have seen that changes in the dynamics, like inclusion of diffusion, multi-particle processes, multiple components, sequential versus parallel updating, do not seem to alter the critical behavior of the models. Several examples confirm that the DP universality class is very robust. The two-component ZGB model exhibits a second-order phase transition of the DP kind [15]. Various cellular automata for surface reactions (simultaneous-update versions of the ZGB model) have been studied [35, 36] and found to have a critical behavior consistent with directed percolation. A basis for universality appears in field theory, providing one can show that the continuum descriptions for various models differ only by irrelevant terms. In field theory the microscopic picture of particles on a lattice is replaced by a set of densities which evolve via stochastic partial differential equations (Langevin equations). Janssen [4] proposed a continuum description of the CP and allied models:

$$\frac{\partial\rho(\vec{x},t)}{\partial t} = a\rho(\vec{x},t) - b\rho(\vec{x},t)^2 - c\rho(\vec{x},t)^3 + \ldots + D\nabla^2\rho(\vec{x},t) + \eta(\vec{x},t), \qquad (2.34)$$

where $\rho(\vec{x},t) \geq 0$ is the particle density; the ellipsis represents terms of higher order in $\rho(\vec{x},t)$. $\eta(\vec{x},t)$ is a gaussian noise, which respects the absorbing state $\rho(\vec{x},t) = 0$, as shown by its autocorrelation:

$$\langle\eta(\vec{x},t)\eta(\vec{x}',t')\rangle \propto \rho(\vec{x},t)\delta(\vec{x}-\vec{x}')\delta(t-t'). \qquad (2.35)$$

The noise term represents fluctuations, which are irregular and unpredictable, arising from the microscopic degrees of freedom. From eq. (2.35) we see that noise is uncorrelated in space and time. Renormalization group analysis of the field theory has shown that at least in the vicinity of the model's upper critical dimension, higher powers of $\rho$ and its derivatives are irrelevant for the critical properties of the system as long as $b > 0$. From the mean-field approximation, in which the noise is dropped, it is clear that the transition out of the absorbing state occurs when $a = 0$. Eq. (2.34) describes a generic phase transition of a noisy system with a single-component order parameter, $\rho(\vec{x}, t)$, into an absorbing state.

The "DP conjecture" asserts that models with a scalar order parameter possessing a continuous phase transition to a unique absorbing state belong generically to the DP universality class [4, 5] or Reggeon field theory [9]. The situation is analogous to $\phi^4$ theory describing the generic ferromagnetic transition in equilibrium Ising models [37, 3].

Despite its robustness, exceptions to the DP conjecture have been reported in the past years. We discuss two important examples, in which models presenting multiple absorbing configurations or obeying conservation laws do not exhibit DP-like critical behavior. An example of a model with multiple absorbing configurations is the pair-contact process (PCP) [39]. In this model pairs, defined as two particles sitting at nearest-neighbor sites, are annihilated with probability $p$, or else create a new particle at a randomly chosen nearest-neighbor site, provided it is vacant. The absorbing state is characterized by the absence of pairs, i.e., any configuration devoid of pairs is absorbing. This model exhibits a second-order phase transition from the absorbing state to an active steady state whose static behavior is DP-like. But surprisingly, in time-dependent simulations (discussed in section 4.4) the spreading exponents are continuously variable [40].

From equilibrium dynamics it is no surprise that conservation laws can determine the dynamic universality class. The same has been found for nonequilibrium critical phenomena; systems obeying certain conservation laws do not present DP-like critical behavior. A good example of this is the branching annihilating random walk (BAW) model [41], which involves particle hopping, annihilation upon contact and creation of new particles at neighboring sites. At each step of the process a particle is selected at random; it may hop to a randomly chosen neighboring site with probability $p$, or with probability $1 - p$, create $n$ new particles at its nearest neighbor sites. Pairwise annihilation occurs whenever a particle arrives at an occupied site, due either to hopping or to branching. The vacuum is the absorbing state. For even $n$, the particle

number is conserved modulo 2 ("parity conservation") and therefore the vacuum is accessible only if the particle number is even. Even-$n$ BAWs exhibit non-DP critical behavior. On the other hand, odd-$n$ BAWs do not obey any conservation law and are found to belong to the DP universality class [42, 43].

## 2.7 Disordered Systems

Real materials are seldom the idealized pure systems that we are used to dealing with in physics. In any real physical application such as surface or interface growth or chemical reactions on surfaces, impurities or defects are present. Magnetic crystals invariably contain defects and nonmagnetic impurities. Liquids are likely to have impurities dissolved in them. Thus it becomes important to understand the effect of disorder on the properties of materials. In this section we discuss some basic aspects of disorder, and the important result known as the Harris criterion [44].

We can distinguish two broad categories of disorder in solid systems, substitutional and structural (or topological) [45]. In a substitutionally disordered system impurities occupy the sites of a regular lattice and translational periodicity of the lattice is not destroyed. This kind of disorder is found in solid alloys [46]. On the other hand, structurally disordered systems have no regular lattice structure. Examples of such systems are the amorphous semiconductors [47].

In substitutional disordered systems a further distinction is allowed, namely *annealed* or *quenched* disorder [48, 49], according to the way it is distributed in the system. In an annealed system the impurity degrees of freedom are in thermal equilibrium with other degrees of freedom. The distribution that describes the annealed disorder is also changing with the temperature or time interval of interest. In quenched random systems the impurities are frozen into a nonequilibrium but random configuration. Randomly distributed impurities or defects do not equilibrate in the temperature range or time interval in which the properties of the system which are of direct interest are changing. The only difference between the annealed and the quenched impurities comes from the difference in the probability distribution. The annealed impurities interact with the host system, hence their probability distribution depends strongly on the system variables. The quenched impurities are fixed, and their probability distribution is not affected by the system, which evolves under conditions imposed by the quenched impurities.

It is also necessary to distinguish between site and bond disorder. Site dilution is typically represented by uncorrelated random variables $\eta_i$ that take the values 0 or

(a) (b)

Figure 2.3: Examples of bond and site dilution; (a) one bond is removed; (b) one site is removed.

1, with

$$\langle \eta_i \rangle = p^s, \tag{2.36}$$

where $\langle\rangle$ denotes an average over the disorder variables $\eta_i$, and $p^s$ is the site concentration. In quenched site disorder the configurational averages are independent of the thermal averages, and weighted by a product of single-site probability densities,

$$P(\eta_i) = (1 - p^s)\delta(\eta_i) + p^s\delta(\eta_i - 1). \tag{2.37}$$

In annealed site disorder the averages of the disorder variables are carried out together with the other variables of the system. In this case disorder variables on different sites are not independent. In bond disordered systems, disorder variables $\eta_{ij}$ are associated with bonds. The probability density for a disorder variable in a system with quenched bond dilution is

$$P(\eta_{ij}) = (1 - p)\delta(\eta_{ij}) + p\delta(\eta_{ij} - 1), \tag{2.38}$$

where $p$ is the bond concentration. It is clear from Fig. (2.3) that site dilution is more effective than bond dilution in disconnecting the lattice. Defining $p_c^b$ as the critical bond concentration and $p_c^s$ as the critical site concentration, it is easy to see that $p_c^s > p_c^b$.

The effect of impurities on critical phenomena has been the subject of many studies. A lot of effort has been made towards understanding how disorder can affect the nature of phase transitions, in particular, whether critical exponents are changed due to disorder. An important result in this connection was made by Harris [44]. The well-known Harris criterion states that a system with quenched disorder presents critical behavior different from that of the corresponding pure model if the exponents

of the pure model satisfy $d\nu_\perp \leq 2$, where $d$ is the spatial dimensionality and $\nu_\perp$ the correlation-length exponent. This relation can be rewritten as $\alpha > 0$, where $\alpha$ is the specific-heat exponent, and we made use of the hyperscaling relation $2 - d\nu_\perp = \alpha$.

A simple and heuristic way to derive the Harris criterion is as follows [50]. One introduces small quenched local fluctuations, of average magnitude $V$ and zero mean, to a pure system, that undergoes a continuous phase transition, at criticality. The summed fluctuation in a Kadanoff block [17] of length $b$ along each dimension will be $b^{d/2}V$. It is reasonable to hypothesize heuristically that this has the same effect as when the summed fluctuation is equally distributed among all the sites inside the block, namely $b^{-d/2}V$ per site. By performing a renormalization group (RG) transformation [18], replacing each block by a single site of the renormalized system, one assumes that the quenched fluctuation associated with the renormalized site is of the same form as the original one. Thus,

$$V' = b^{y_V} b^{-d/2} V, \tag{2.39}$$

where $y_V$ is the eigenvalue exponent of the pure system corresponding to the variable which is being perturbed by the quenched fluctuations. In RG terms, we are "measuring" whether disorder is a relevant variable at the critical point of the pure system. Thus if $y_V - d/2$ is positive the eigenvalue is relevant, meaning that the system flows away from the pure fixed point. Otherwise the eigenvalue is irrelevant and the pure fixed point stable. It is interesting to remark that when $V$ is a bond strength, the exponent $y_V$ is the reciprocal of the correlation length $\nu_\perp$, and the criterion is equivalent to the sign of the specific-heat exponent $\alpha$. When $V$ is a magnetic field, the criterion is equivalent to the sign of the susceptibility exponent $\gamma$.

# Chapter 3

# Diluted Contact Process - Mean-field Theory

## 3.1 Introduction

Many-particle systems often incorporate a degree of frozen-in randomness, due to nonuniformities in structure and composition, which can drastically alter their cooperative behavior. For simple systems such as the Ising model, much effort has been devoted to exploring the effect of quenched disorder on the phase diagram, the order of the transition, and on the critical exponents [51, 44].

In this chapter we examine the effect of quenched disorder on a nonequilibrium system undergoing a continuous phase transition to an absorbing state. Such transitions have attracted widespread attention, due to their relevance to diverse physical processes (catalysis, transport in random media), and to issues bearing on universality. We focus on the two-dimensional contact process (CP), a simple lattice model of an epidemic [1]. Disorder is introduced by randomly removing sites from the lattice with a certain probability. The pure CP presents a second-order phase transition characterized by critical exponents that belong to the directed percolation (DP) universality class. The well-known Harris criterion [44] states that disorder changes the critical exponents of a model if the exponents of the pure system satisfy $d\nu_\perp \leq 2$, where $d$ is the dimensionality and $\nu_\perp$ the correlation-length exponent. Since $\nu_\perp \simeq 0.73$ for DP in 2+1 dimensions, we expect that the diluted contact process (DCP) will present critical behavior different from that of the pure CP.

The chapter is organized as follows. In the next section we define the diluted model. In section (3.3) we study the DCP through mean-field cluster approximations.

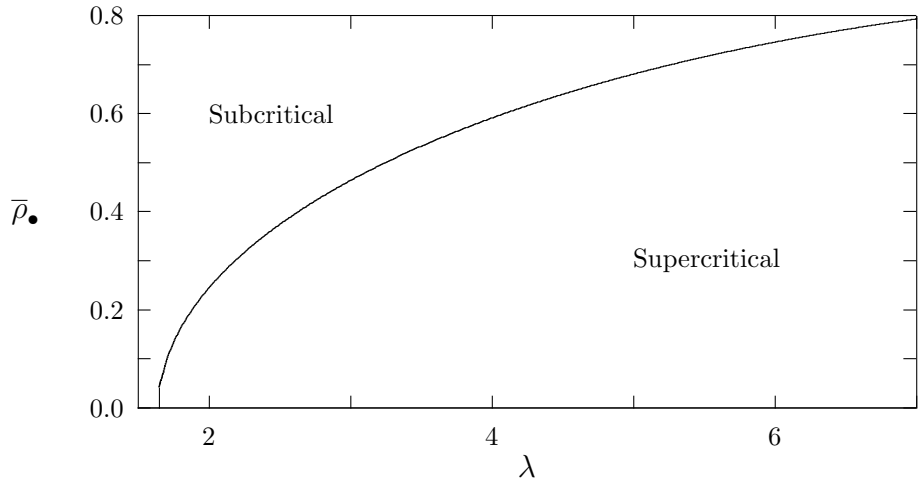


Figure 3.1: Steady-state concentration of particles as a function of the creation parameter. For $\lambda < \lambda_c(0)$ the system is in the subcritical region, and for $\lambda > \lambda_c(0)$ the system is in the supercritical region.

In section (3.4) we present our concluding remarks.

## 3.2 The Model

The CP, a continuous time Markov process, originally introduced by Harris [1] as an epidemic model, can be seen as a model for creation and annihilation of particles on a lattice. Each site of $\mathbf{Z}^2$ is either vacant or occupied. In order to get the Markov property we use exponential distributions to describe the evolution of the process [52]. Particles wait a mean time $\lambda$ and then give birth at nearest neighbor vacant sites. A particle waits a mean time of unity before dying. The order parameter is the stationary density $\overline{\rho}_\bullet$ (the bar denotes a stationary value); it vanishes in the vacuum state, which is absorbing. As $\lambda$ is increased beyond $\lambda_c(0) = 1.6488(1)$[1], the model presents a continuous phase transition from the vacuum to an active steady state [2, 7, 53]. Fig. (3.1) represents the phase diagram of the two-dimensional CP. For $\lambda < \lambda_c(0)$ any system with a finite population enters the absorbing state with probability 1, and for $\lambda > \lambda_c(0)$ there is a nonzero probability that the system survives as $t \to \infty$. The critical behavior of the pure CP is characterized by the same critical exponents as directed percolation (DP) [22].

[1]This value is obtained through simulations, refer to Ch.4

We introduce disorder by randomly removing sites from the lattice with probability $x$. That is, for each $(i,j) \in \mathbf{Z}^2$ there is an independent random variable $\eta(i,j)$, taking values of 0 and 1 with probabilities $x$ and $1-x$, respectively. If $\eta(i,j) = 0$ this site may never be occupied. Thus if exactly $m$ neighbors of a given site have $\eta(i,j) = 1$, the creation rate at that site is at most $m\lambda/4$. Naturally, $1-x$ must exceed the percolation threshold ($p_c = 0.5927$), otherwise the lattice will break into disconnected islands.

## 3.3 Mean–field Cluster Expansions

Mean-field theory may be considered the simplest analytical method which has been successfully employed in the study of many-particle systems. In this section we approach the diluted model through mean-field cluster expansions. We begin this section by indicating the general scheme for $(n,m)$-approximations. Then we apply the one-site approximation to the diluted contact process and finally, we improve the results by applying the pair-approximation.

### 3.3.1 $(n,m)$-Cluster Approximation

Cluster expansion is a natural way to improve the mean-field approach. The basic idea consists of treating the transitions inside these clusters exactly, while the interactions with sites outside a cluster is mean-field like. We follow the generalization scheme studied by ben-Avraham and Köhler [23], the $(n,m)$-approximation. In this description the parameter $n$ indicates the cluster size and $m$ its overlap with other clusters.

The building blocks of the cluster method are the probabilities, $\rho_{x_1 x_2 \cdots x_j}$, that any $j$ consecutive sites be in the states $x_1, x_2, \cdots, x_j$. Any lattice model can be defined in terms of $j$-cluster processes. In this expansion the evolution equation for a two-site cluster involves three-site clusters; similarly an equation for a three-site cluster involves four-site ones; and so on. Following this reasoning we end up with an infinite hierarchy of rate equations for increasing cluster sizes. The method consists in cutting off this hierarchy at some order $n$ by approximating large cluster probabilities in terms of the $n$-site cluster probabilities. The simplest approximation, $(n,0)$, ignores the correlations between the first $n$ sites and the sites to their right,

$$\rho_{x_1 x_2 \cdots x_n x_{n+1} \cdots} = \rho_{x_1 x_2 \cdots x_n} \rho_{x_{n+1} \cdots} \tag{3.1}$$

The next step in this expansion is to consider an overlap of one site between adjacent clusters. The $(n, 1)$-approximation,

$$\rho_{x_1 x_2 \cdots x_n x_{n+1} \cdots} = \rho_{x_1 x_2 \cdots x_n} \frac{\rho_{x_n x_{n+1} \cdots}}{\rho_{x_n}} \tag{3.2}$$

is given by the product between the probability that the $n$ first sites be in the states $x_1, x_2, \cdots, x_n$ and the conditional probability of having a cluster in state $x_n x_{n+1} \cdots$, given that site $n$ is in state $x_n$, which is simply expressed as a ratio of probability, according to Bayes' rule. In general we may allow for an overlap of $m$ sites, restricting $0 \leq m \leq n-1$, yielding the $(n, m)$-approximation,

$$\rho_{x_1 x_2 \cdots x_n x_{n+1} \cdots} = \rho_{x_1 x_2 \cdots x_n} \frac{\rho_{x_{n-m+1} x_{n-m+2} \cdots x_n x_{n+1} \cdots}}{\rho_{x_{n-m+1} x_{n-m+2} \cdots x_n}} \tag{3.3}$$

In order to illustrate the technique let us consider a six-cluster in the state $ABCDEF$. In the $(3, m)$-approximations the probability of such a cluster would be given by:

$$\rho_{ABCDEF} = \rho_{ABC} \rho_{DEF} \tag{3.4}$$

in the $(3, 0)$-approximation, without overlap;

$$\rho_{ABCDEF} = \rho_{ABC} \frac{\rho_{CDE}}{\rho_C} \frac{\rho_{EF\bullet}}{\rho_E} \tag{3.5}$$

in the $(3, 1)$-approximation, where $\bullet$ indicates an unspecified site; and finally

$$\rho_{ABCDEF} = \rho_{ABC} \frac{\rho_{BCD}}{\rho_{BC}} \frac{\rho_{CDE}}{\rho_{CD}} \frac{\rho_{DEF}}{\rho_{DE}} \tag{3.6}$$

in the $(3, 2)$-approximation. Notice that only the latter expression, eq. (3.6), satisfies translation invariance automatically. This is a characteristic of the $(n, n-1)$-approximations, which yield the most accurate results [23]. In the other approximations, $m < n-1$, one should be careful to account for all possible combinations and to preserve thereby the fundamental property of translation invariance. In the $(3, 0)$-approximation, $\rho_{ABCDEF}$ could also be well represented by $\rho_{\bullet AB} \rho_{CDE} \rho_{F\bullet\bullet}$ or by $\rho_{\bullet\bullet A} \rho_{BCD} \rho_{EF\bullet}$.

Implicit in this method is the assumption that the system is translationally symmetric; cluster probabilities are independent of the position of the cluster on the lattice. This symmetry introduces linear relations among the $n$-cluster probabilities. The normalization condition, written in a general form, is given by

$$\sum_{x_1, x_2, \cdots, x_n} \rho_{x_1, x_2 \cdots x_n} = 1. \tag{3.7}$$

A lattice model may impose natural constraints on the accessible states of clusters. The ZGB model [12] for oxidation of carbon monoxide on a catalytic surface, in which molecules of $CO$ and $O$ combine to form $CO_2$, is an example where $CO - O$ pairs are forbidden. It is interesting to remark that this restriction is not taken into account in the site-approximation level.

### 3.3.2 Site-approximation

Let $\sigma_{(i,j)}$ describe the state of the $(i,j)$-site, which can be $\bullet$ (occupied by a particle), $\circ$ (vacant) or $*$ (a removed site). The model is described by the evolution equation,

$$\frac{d\rho_\bullet}{dt} = -\rho_\bullet + \frac{\lambda}{4}\sum_{e=\pm 1}[P(\sigma_{(i,j)} = \circ, \sigma_{(i+e,j)} = \bullet; t) + P(\sigma_{(i,j)} = \circ, \sigma_{(i,j+e)} = \bullet; t)] \quad (3.8)$$

where $e$ can take the values $\pm 1$ and indicates the nearest neighbors of $(i,j)$-site; $\rho_\bullet \equiv \rho_\bullet(i,j;t) \equiv P(\sigma_{(i,j)} = \bullet; t)$ is the probability that site $(i,j)$ is occupied at time $t$, and $P(\sigma_{(i,j)} = \circ, \sigma_{(i,j+e)} = \bullet; t)$ is the joint probability that site $(i,j)$ is vacant and site $(i, j+e)$ is ocuppied at time $t$. To solve Eq. (3.8) we need to know the two-site probabilities appearing on the rhs, which in turn depend on the three-site probabilities, and so forth, leaving us with a hierarchy of equations for the $n$-site probabilities. The site-approximation consists in truncating this hierarchy at $n = 1$, so that the two-site probabilities are replaced by a product of two one-site probabilities. Assuming spatial homogeneity we obtain the following evolution equation for $\rho_\bullet$,

$$\frac{d\rho_\bullet}{dt} = [\lambda(1-x) - 1]\rho_\bullet - \lambda\rho_\bullet^2 \quad (3.9)$$

where $x$ is the concentration of removed sites. For $\lambda(1-x) \leq 1$ the only stationary solution is $\overline{\rho}_\bullet = 0$. For $\lambda(1-x) > 1$ we also find an active stationary solution, namely $\overline{\rho}_\bullet = 1 - x - 1/\lambda$. In spite of the simplicity of this approximation, we detect the existence of a continuous phase transition from an active steady state ($\overline{\rho}_\bullet \neq 0$) to an absorbing one ($\overline{\rho}_\bullet = 0$), at $\lambda_c(x) = 1/(1-x)$. Setting $x = 0$, we naturally recover the site-approximation result for the regular CP, $\lambda_c(0) = 1$.

### 3.3.3 Pair-approximation

The next step in this analysis is the pair approximation, in which we only take into account correlations between nearest neighbor sites. Thus we must consider a 5-site cluster, focusing on the central site (see diagram in Fig. (3.2)). We have a total of seven variables, namely, $\rho_{\bullet\bullet}$, the concentration of ($\bullet\bullet$) pairs; $\rho_{\bullet\circ}$, the concentration of

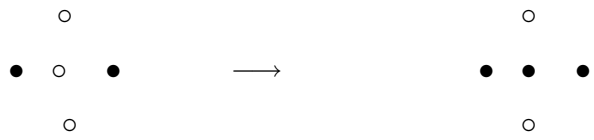

Figure 3.2: Diagram showing a creation event for the two-dimensional contact process.

($\bullet\circ$) pairs and so on; and two constants, $\rho_* \equiv x$ and $\rho_{**}$. The single site concentrations $\rho_\bullet, \rho_\circ$ and $x$, are given by relations such as:

$$\rho_\bullet = \rho_{\bullet\bullet} + \rho_{\bullet\circ} + \rho_{\bullet *}, \tag{3.10}$$

where $\rho_{\bullet\circ} = \rho_{\circ\bullet}$, etc., by symmetry. Similar relations hold for $\rho_\circ$ and $x$. In addition we have normalization,

$$\rho_\bullet + \rho_\circ + x = 1. \tag{3.11}$$

Thus we are left with 3 independent variables. The method consists in writing and solving the evolution equations for the pair concentrations. Joint probabilities of three or more events are expressed as products of the pair concentrations. To see how these equations are constructed, consider the event illustrated in Fig. (3.2). Creation occurs at the central site at rate $\lambda/2$; and the probability of finding the cluster in this sort of configuration is $6P(\sigma_{(i,j)} = \circ)[P(\sigma_{(i\pm1,j)} = \bullet|\sigma_{(i,j)} = \circ)P(\sigma_{(i,j\pm1)} = \circ|\sigma_{(i,j)} = \circ)]^2$. In terms of the pair concentration variables it becomes $6\rho^2_{\bullet\circ}\rho^2_{\circ\circ}/\rho^3_\circ$. The rate of change of $\rho_{\bullet\bullet}$ due to this process is $3\lambda\rho^2_{\bullet\circ}\rho^2_{\circ\circ}/\rho^3_\circ$ times the change in the number of ($\bullet\bullet$) pairs $\Delta N_{\bullet\bullet} = 2$. Perfoming the same sort of calculation for all possible five-site clusters and summing over all processes, we obtain

$$\frac{d\rho_\bullet}{dt} = -\rho_\bullet + \lambda\rho_{\bullet\circ} \tag{3.12}$$

$$\frac{d\rho_{\bullet\bullet}}{dt} = -2\rho_{\bullet\bullet} + \lambda\rho_{\bullet\circ} + \frac{3}{2}\lambda\frac{\rho^2_{\bullet\circ}}{\rho_\circ} \tag{3.13}$$

$$\frac{d\rho_{\circ\circ}}{dt} = -2\rho_{\bullet\circ} + \frac{3}{2}\lambda\frac{\rho_{\bullet\circ}\rho_{\circ\circ}}{\rho_\circ} \tag{3.14}$$

$$\frac{d\rho_{\bullet *}}{dt} = -2\rho_{\bullet *} + \frac{3}{2}\lambda\frac{\rho_{\bullet\circ}\rho_{\circ *}}{\rho_\circ} \tag{3.15}$$

where some variables were eliminated using equations (3.10) and (3.11). After some algebra we obtain the following equation for the stationary density,

$$\overline{\rho}^2_\bullet(1-3\lambda) \;+\; \overline{\rho}_\bullet(15\lambda - 27\lambda x - 8 - 8x + 12\lambda\rho_{**})$$

| x | 0.02 | 0.05 | 0.1 | 0.2 | 0.3 | 0.35 |
|---|---|---|---|---|---|---|
| MFT | 0.020 | 0.053 | 0.111 | 0.250 | 0.428 | 0.538 |
| Simulations | 0.022 | 0.056 | 0.119 | 0.278 | 0.498 | 0.649 |

Table 3.1: The ratio $[\lambda_c(x) - \lambda_c(0)]/\lambda_c(0)$ for critical parameters obtained through mean-field theory and simulations.

$$+ \quad 16(1-x)^2 + 12\lambda(3x - 2x^2 - \rho_{**} + \rho_{**}x - 1) = 0. \qquad (3.16)$$

Solving Eq. (3.16) for $\overline{\rho}_\bullet$ and setting $\overline{\rho}_\bullet = 0$, we get

$$\lambda_c(x) = \frac{4(1-x)}{3(1-2x+\rho_{**})} \, . \qquad (3.17)$$

By setting $x = 0$ we recover the pair-approximation result for the regular CP, $\lambda_c(0) = 4/3$. Since sites are removed independently, $\rho_{**} = x^2$, and Eq. (3.17) becomes

$$\frac{\lambda_c(x)}{\lambda_c(0)} = \frac{1}{(1-x)}. \qquad (3.18)$$

Thus the relative shift in the critical point $[\lambda_c(x) - \lambda_c(0)]/\lambda_c(0)$ shows the same dependence on dilution concentration in both the site- and pair-approximations. This suggests that Eq. (3.18) may provide a reasonable estimate. In table 3.1 the shifts $[\lambda_c(x) - \lambda_c(0)]/\lambda_c(0)$ are listed for different dilution concentrations. As we can see there is fair agreement between simulation and MFT, as long as $1 - x$ is well above the square-lattice site percolation threshold, $p_c \simeq 0.5927$. (Simple mean-field theories do not detect the breakdown of connectivity for $1 - x < p_c$.)

## 3.4 Discussion

It is well-known that mean-field cluster expansions generally provide qualitatively correct descriptions of phase diagrams. Based on our results, cluster expansions predict a continuous absorbing-state transition in the diluted contact process at $\lambda_c(x)$. They yield a critical parameter that depends on the dilution, $x$. In fact a similar result was also found by Marques [25] in a mean-field renormalization group study of the effects of dilution on the contact process and related models. (Marques considers a diluted model slightly different from ours). We believe that the relation, $\lambda_c(x) \sim \lambda_c(0)/(1-x)$, yielded by site- and pair-approximations, gives the correct picture of this dependence

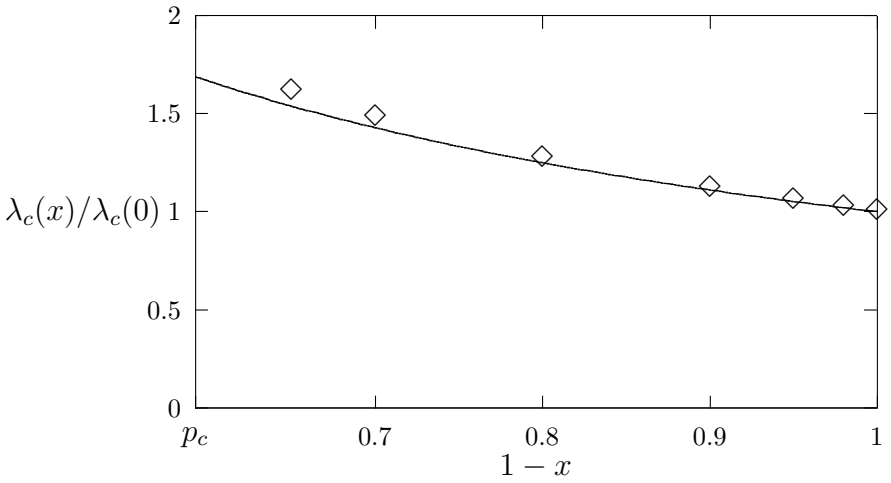


Figure 3.3: $\lambda_c(x)/\lambda_c(0)$ versus $(1-x)$; the full curve represents the mean-field results, and the $\diamond$ the simulation values.

as long as $x << 1-p_c$. A plot of $\lambda_c(x)/\lambda_c(0)$ versus $(1-x)$, Fig. (3.3), for simulation and mean-field results, support this conjecture. Dilution has the effect of increasing the critical parameter; this increase is the way the system balances the creation inhibition caused by removing sites from the lattice, consequently reducing the number of effective neighbors. On the other hand, this technique yields poor quantitative results for critical exponents. This is expected to happen as we neglect correlations in systems that are highly correlated.

From Fig. (3.3) we notice that the critical parameter, $\lambda_c$, for the contact process on a percolation cluster $(1-x=p_c)$ is finite. Indeed, the critical parameter $\lambda_c(x=1-p_c)$ must be less than or equal to $\lambda_c(x=0)$ for the *one-dimensional* contact process. This happens as a consequence of the strong dependence of the critical parameter on the number of occupied neighbors. In one dimension, sites have but two occupied neighbors, while in the backbone of an incipient percolation cluster, lots of sites might have more than two occupied neighbors. Thus, the critical parameter of the one-dimensional CP serves as an upper limit for the CP in the percolation cluster $(\lambda_c(x=1-p_c) \leq 3.29771)$ [27].

In our MFT calculations we represented the quenched dilution condition by not allowing the $n$-point probabilities for removed sites to evolve with time. It is important to point out that this can also represent a problem in which the probability distribution of *annealed* dilution does not evolve with time. We hope to improve this

in future work.

# Chapter 4

# Diluted Contact Process - Simulations

## 4.1 Introduction

The present chapter is best viewed as a continuation of the previous one. Here we study the diluted contact process via numerical methods. We obtain the critical parameter and exponents pertinent to critical behavior through Monte Carlo simulations. Numerical simulations have been shown to be very useful in the understanding of nonequilibrium phase transitions, exact solutions are generally impossible, and very laborious in the rare instances where they are feasible. As we will see, simulations are not straightforward either, and require a number of tricks in order to provide accurate results.

We start this chapter by describing the diluted contact process (DCP) in its discrete version. In section (4.3) we consider simulations of the steady-state behavior. Then we study the time-dependent properties in section (4.4). In section (4.5) we review the nonexponential relaxation to the vacuum of the survival probability. Concluding remarks are presented in section (4.6).

## 4.2 The Model

The CP is a model for creation and annihilation of particles on a lattice, in which each site can either be occupied by a particle or vacant. Although the CP is a continuous-time Markov process, it is possible to define a discrete-time formulation, which is often employed in simulations [13]. The discrete and continuous-time formulations

differ somewhat at short times, but they share the same stationary properties and long-time dynamics. In the discrete version one step consists of first choosing a site randomly. Then if it is occupied either of the processes may take place: annihilation with probability $1/(1+\lambda)$, or creation at a randomly chosen nearest neighbor (if it is vacant), with probability $\lambda/(1+\lambda)$. If the site chosen initially is vacant, nothing happens. After each step (successful or not) time is advanced by a fixed increment, $\Delta t$. (It is conventional to set $\Delta t = 1/N$, where $N$ is the total number of sites, since this implies an average of one event per site, per unit time). A great improvement in efficiency is obtained by choosing from a list of occupied sites. This avoids the waste of time associated with the large proportion of rejected trials, when the density of particles is low. When the initial site is chosen from the list of all $N_{occ}$ occupied sites, the time increment should be defined as $\Delta t = 1/N_{occ}$.

We introduce disorder by randomly removing a fraction $x$ of the sites. That is, for each $(i,j) \in \mathrm{Z}^2$ there is an independent random variable $\eta(i,j)$, taking values 0 and 1 with probability $x$ and $1-x$, respectively. The DCP is simply the contact process restricted to sites with $\eta(i,j) = 1$; sites with $\eta(i,j) = 0$ may never be occupied. Naturally, $1-x$ must exceed the percolation threshold $p_c = 0.5927$ for there to be any possibility of an active state, since on any finite set the CP is doomed to extinction.

Each trial is generated as follows. We first initialize the lattice by randomly removing sites accordingly to a preset dilution. Then we define an initial particle distribution which depends on the kind of properties we intend to study. We let the process evolve, annihilation and creation of particles take place, until a maximum time $t_{max}$. Once this trial is complete, we start a new one by setting the same initial particle distribution, but generating a new set of disorder. An independent realization of disorder (the variables $\eta(i,j)$), is generated for each trial, and thus we perform an average over disorder. As critical points are characterized by power-law divergencies of the correlation length and the relaxation time, one has to study large systems over long times to obtain reliable results.

## 4.3 Steady-state Behavior

In order to perform a steady-state analysis, we start out with the system in a state far from the absorbing state. For the DCP we initialize the lattice with a dense configuration, all sites occupied ($\rho_\bullet = 1-x$, at $t = 0$). Then we allow it to evolve

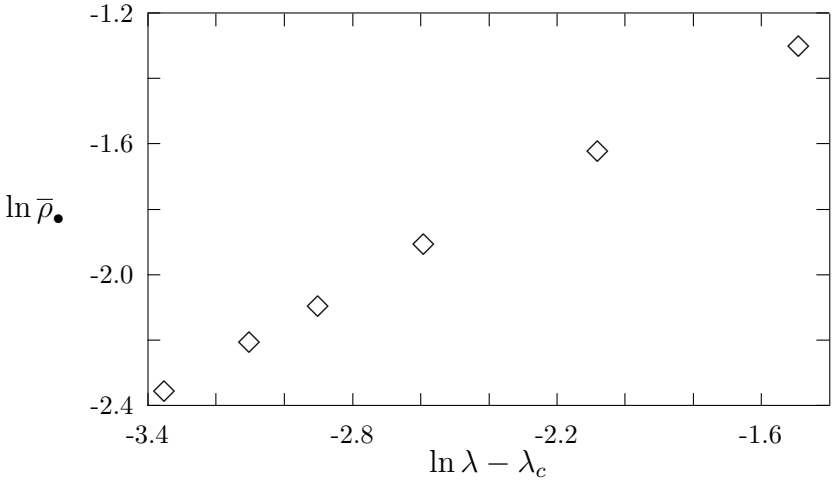


Figure 4.1: Log-log plot of the stationary density vs. $(\lambda - \lambda_c)$ for $x = 0.02$.

according to its dynamics until, after a relaxation time $\tau$, the steady state [1] is reached. Once in the steady state one measures the density of particles ($\overline{\rho}_\bullet$, where the bar indicates a stationary value) at various time intervals up to $t_{max}$ thus performing a time average. As we have seen, the density of particles in the active state goes to zero when $\lambda \to \lambda_c+$ as

$$\overline{\rho}_\bullet \sim \Delta^\beta, \tag{4.1}$$

where $\Delta \equiv \lambda - \lambda_c$ and $\beta$ is the critical exponent associated with the order parameter. Log-log plots of the order parameter *versus* $\Delta$ should provide a straight line whose slope is the critical exponent $\beta$.

### 4.3.1 Simulation Results

The results for $\overline{\rho}_\bullet$ were obtained by averaging over typically 50 to 100 independent samples. The number of time steps $t$ and system sizes $L$ varied from $t = 1000, L = 32$ far from $\lambda_c$ to $t = 6000, L = 128$ to closest to $\lambda_c$. To evaluate $\Delta$ we must of course have an accurate value of $\lambda_c(x)$; in this study we use the values given in Table 4.2. In section (4.4) we explain the method we use to determine the critical parameters.

In Fig. (4.1) we plot $\overline{\rho}_\bullet \times \Delta$ for $x = 0.02$, and using $\lambda_c = 1.6850(3)$. It is clear from this picture that the power-law behavior of eq. (4.1) is confirmed. Furthermore, it can also be taken as a confirmation that $\lambda_c = 1.6850(3)$ marks a critical point.

[1] Instead of steady state, we would rather use "quasi-steady state" as the system only attains an active steady state in an infinite-size system.

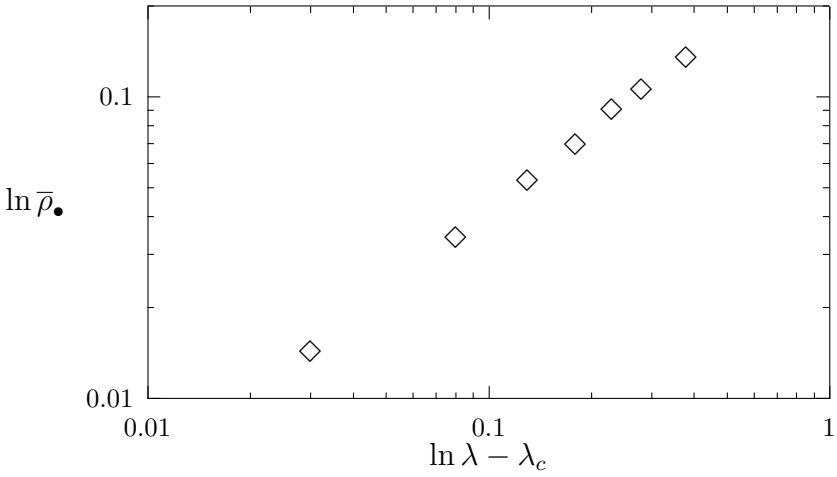


Figure 4.2: Log-log plot of $\overline{\rho}_\bullet$ vs. $(\lambda - \lambda_c)$ for $x = 0.35$.

We estimate $\beta = 0.566(7)$ where the figure in parenthesis indicates the estimated uncertainty in the last digit. This result for $\beta$ is in good agreement with the typical estimates for directed percolation in $(2+1)$ dimensions, $\beta = 0.586(14)$ [54]. Following the same procedure, we estimate $\beta = 0.89(1)$ for $x = 0.35$, as shown in Fig. (4.2).

## 4.4 Time-dependent Behavior

### 4.4.1 Scaling Ansatz

We consider from now on asymptotic distributions of configurations starting off at $t = 0$ with one particle at the origin. In the scaling regime, i.e., very close to the critical point, at long times and in large systems, there is a unique dominant length scale $\xi$ and time scale $\tau$. According to the scaling hypothesis, one expects that properties such as the local density $\rho_\bullet(\mathbf{x}, t)$ or the survival probability $P(t)$, depend on the relevant parameters $\mathbf{x}, t$ and $\Delta$, only through the scaling variables $\mathbf{x}^2/t^z$ and $\Delta t^{1/\nu_\parallel}$, times some power of $\mathbf{x}^2, t$ or $\Delta$. The dependence on position, $\mathbf{x}$, is demanded by symmetry and the growth of the characteristic length scale $\propto t^{z/2}$ (note however that $z$ is not the critical exponent of dynamic critical phenomena); the time-dependence involves the ratio $t/\tau$, since $\tau \propto \Delta^{-\nu_\parallel}$ [13]. Thus, in the scaling regime, the local particle density, averaged over all trials, surviving or not, can be written as

$$\rho_\bullet(\mathbf{x}, t) \simeq t^{\eta - dz/2} F(\mathbf{x}^2/t^z, \Delta t^{1/\nu_\parallel}), \tag{4.2}$$

and for the survival probability, the probability that the system has not reached the absorbing state at time $t$, we expect

$$P(t) \simeq t^{-\delta}\phi(\Delta t^{1/\nu_\parallel}). \tag{4.3}$$

$\eta$ and $\delta$ are further critical exponents, while $F$ and $\phi$ are scaling functions. Using Eq. (4.2), we get for the mean number of particles $n(t)$ and the mean-square distance of spreading $R^2(t)$,

$$\begin{aligned} n(t) &= \int d^d x \rho_\bullet(x,t) \propto t^\eta f(\Delta t^{1/\nu_\parallel}), \\ R^2(t) &= \frac{1}{n(t)} \int d^d x x^2 \rho_\bullet(x,t) \propto t^z g(\Delta t^{1/\nu_\parallel}). \end{aligned} \tag{4.4}$$

From eqs.(4.3) and (4.4) it is easy to see that if the functions $\phi(y), f(y)$ and $g(y)$ are nonsingular at $y = 0$, the asymptotic behavior of $P(t), n(t)$ and $R^2(t)$ as $t \to \infty$, at the critical point, determines the critical exponents $\delta, \eta$ and $z$:

$$\begin{aligned} P(t) &\propto t^{-\delta}, \\ n(t) &\propto t^\eta, \\ R^2(t) &\propto t^z. \end{aligned} \tag{4.5}$$

The asymptotic behavior of the scaling functions for $\Delta t^{1/\nu_\parallel} \to -\infty$ is obtained by noting that far from the critical point correlations are short-ranged. Thus, in the subcritical region, $\lambda < \lambda_c$, $P(t)$ and $n(t)$ decay exponentially, while $R^2(t) \propto t$, as if particles diffused on the lattice. In the supercritical regime, $\lambda > \lambda_c$, there must be a nonzero chance of survival, $P_\infty \equiv \lim_{t\to\infty} P(t) > 0$; the active region expands into the vacuum at a constant rate, so that $n(t) \propto t^d$ in $d$ dimensions and $R^2(t) \propto t^2$. Still considering the $\Delta > 0$ region, we see that by setting $\psi(\zeta) = \zeta^{-\delta\nu_\parallel}\phi(\zeta)$ we may rewrite eq. (4.3) as

$$P(t) \propto \Delta^{\delta\nu_\parallel}\psi(\Delta t^{1/\nu_\parallel}). \tag{4.6}$$

Since $P_\infty$ is finite, $\lim_{\zeta\to\infty}\psi(\zeta)$ is finite too, and we get $P_\infty \sim \Delta^{\delta\nu_\parallel}$. It can be shown that the ultimate survival probability and the stationary particle density have the same critical exponent [22]. Hence as $\overline{\rho}_\bullet \propto \Delta^\beta$, we must have the following scaling relation

$$\beta = \delta\nu_\parallel. \tag{4.7}$$

Let us consider next the local density at any fixed $\mathbf{x}$. In the limit $t \to \infty$ and for $\Delta > 0$,

$$\rho_\bullet(\mathbf{x}, t) \to P_\infty \overline{\rho}_\bullet \propto \Delta^{2\beta}, \tag{4.8}$$

since $\rho_\bullet(\mathbf{x}, t)$ in eq. (4.2) represents the density averaged over all trials. From eq. (4.2) we see that $F(0, \Delta t^{1/\nu_\parallel}) \propto \Delta^{2\beta} t^{2\beta/\nu_\parallel}$, for $\Delta t^{1/\nu_\parallel}$ large and positive. Thus we get

$$\rho_\bullet(\mathbf{x}, t) = t^{\eta - dz/2} \Delta^{2\beta} t^{2\beta/\nu_\parallel}. \tag{4.9}$$

In order to remove the overall $t$-dependence we must have

$$4\delta + 2\eta = dz, \tag{4.10}$$

where we used $\beta = \delta\nu_\parallel$. This expression is known as the hyperscaling relation as it relates the dimensionality to critical exponents. It is expected to hold for $d \leq d_c$. Further scaling relations among critical exponents can be found in [13].

### 4.4.2 Simulation Results

We studied dilutions $x = 0.02$, 0.05, 0.1, 0.2, 0.3, and 0.35, on square lattices of 2200 sites to a side, using samples of from $10^4$ to $2 \times 10^6$ trials for each $\lambda$ value of interest, each trial extending to a maximum time of $t_{max} \leq 2 \times 10^6$. As is usual in this sort of simulation, the time increment associated with an elementary event — creation or annihilation — is $\Delta t = 1/N$, where $N$ is the number of particles. The largest samples and longest runs were used at or near critical. An independent realization of disorder (the variables $\eta(i, j)$), is generated for each trial.

In Fig. (4.3) we show log-log plots of $P(t), n(t)$ and $R^2(t)$, as functions of $t$ for dilution $x = 0.02$. The plot illustrates these quantities at both critical and off-critical values. For $\lambda = 1.68$ we see that $n(t)$ and $P(t)$ show a negative curvature, indicating that this parameter is subcritical. In the same way, we see a positive curvature for the supercritical value $\lambda = 1.69$. The power-law behavior as predicted by eq. (4.5) at the critical point is found for $\lambda = 1.685$. Notice that the plot for $n(t)$ is more sensitive to the changes in $\lambda$, showing a more pronounced curvature for the sub and supercritical parameters. We will see that the same is true for the local slope plots. A more accurate determination of the critical point is afforded by analyzing the local slopes $\delta(t)$, $\eta(t)$, and $z(t)$ which are given by

$$-\delta(t) = \frac{\ln[P(t)/P(t/m)]}{\ln(m)}, \tag{4.11}$$

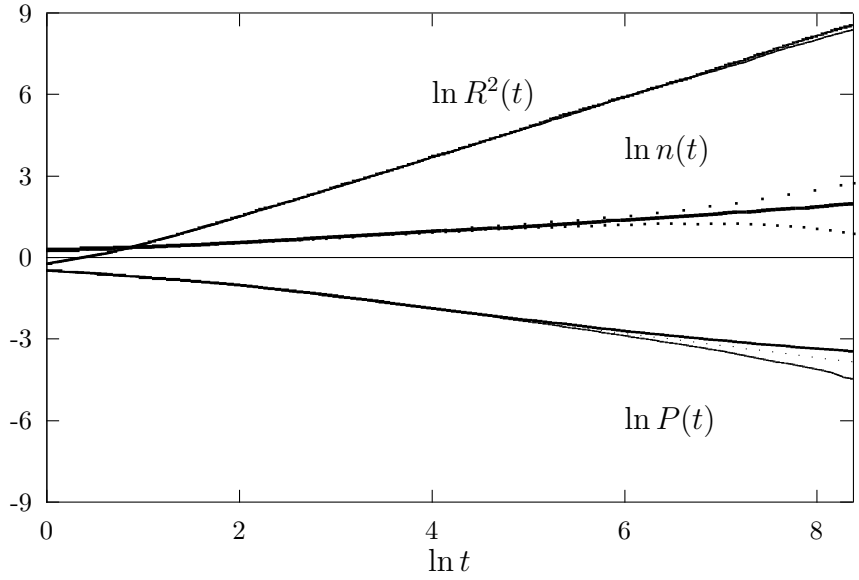


Figure 4.3: Log-log plots of $P(t), n(t)$ and $R^2(t)$ versus $t$ for $x = 0.02$. In each plot, from bottom to top, we have $\lambda = 1.68; 1.685; 1.69$.

where $m$ is a fixed integer. Analogous expressions hold for $\eta(t)$ and $z(t)$. In the present work we compute the local slopes by using least-squares fits to the data (in a logarithmic plot), distributed symmetrically about a given $t$ (typically in the interval $[t/3,\ 3t]$). We estimate the exponents by plotting the local slopes versus $1/t$ and extrapolating to $1/t \to 0$ [8]. In Fig. (4.4) we plot the corresponding local slopes for $x = 0.02$. In plots of the local slopes *versus* $1/t$ one sees that the curves for the off-critical values of $\lambda$ veer up or down, in the supercritical or subcritical regime, respectively. We estimate the critical parameter $\lambda_c$ for $x = 0.02$ by looking at the curvature of the $\eta(t)$ and $\delta(t)$ plots. Both yield the best estimate $\lambda_c = 1.685(5)$. More detailed results indicate that $\lambda_c(x = 0.02)$ is in fact 1.6850(3), see Table 4.2. For the critical exponents we get $\delta = 0.467(1); \eta = 0.216(3)$; and $z = 1.104(2)$.

For dilution $x = 0.02$ the DCP exhibits a pure-CP behavior even at very long times. The same is not true when considering a higher degree of disorder. In Fig. (4.5) we plot $P(t), n(t)$ and $R^2(t)$ as a function of $t$ (in a logarithmic scale) for $x = 0.3$ and different values of $\lambda$. For the DCP we expect the survival probability to exhibit a power-law decay in the *subcritical regime*, in a phenomenon similar to the one responsible for the Griffiths phase. In the Griffiths phase the long-time dynamics are governed by atypical regions in which the fraction of diluted sites is low, rendering the process locally supercritical [59]. Briefly, the argument for power-law relaxation

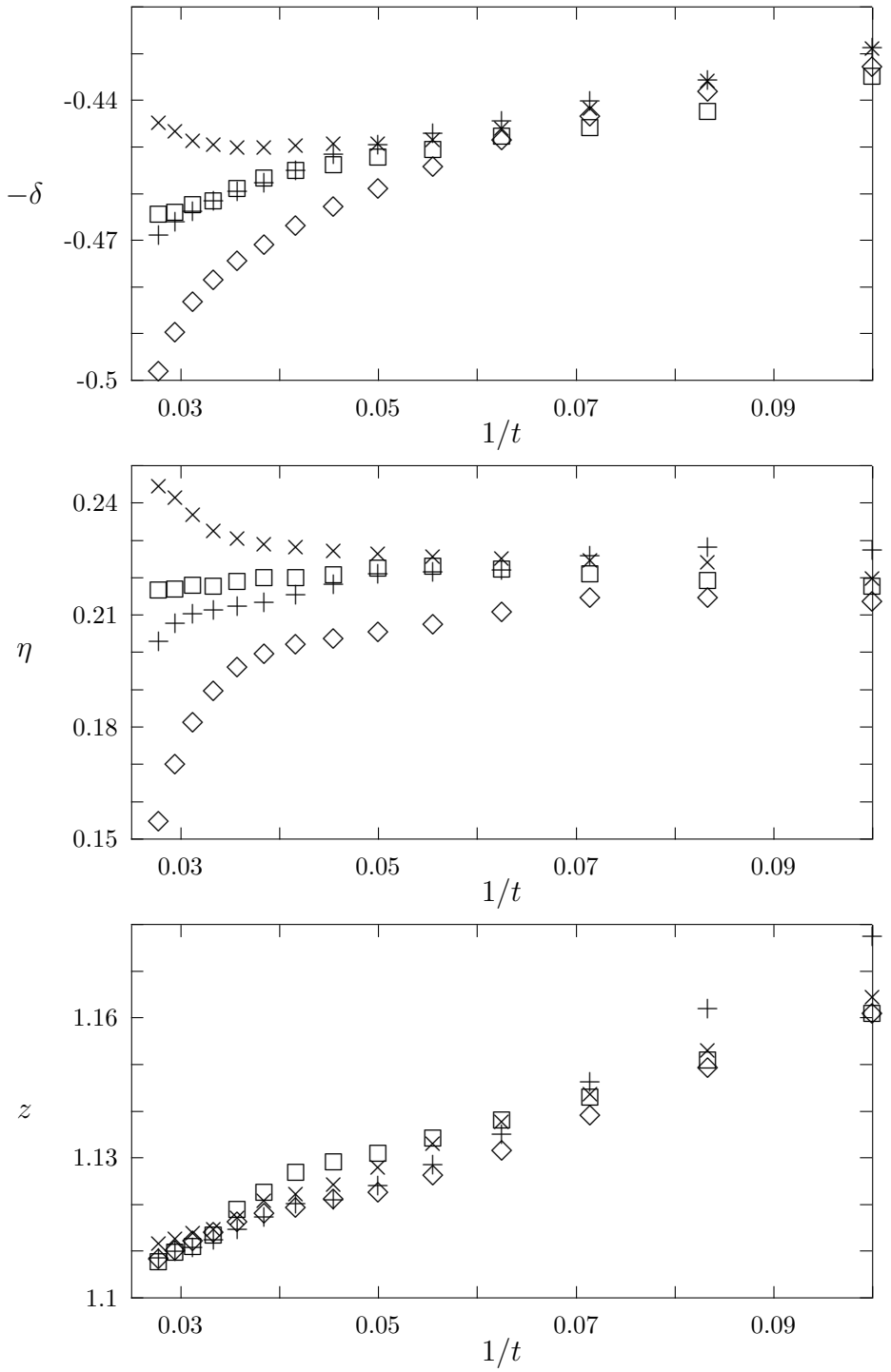


Figure 4.4: Plots of local slopes for $x = 0.02$ and $\lambda = 1.683(\diamond)$; $1.6845(+)$; $1.685(\square)$; $1.6855(\times)$.

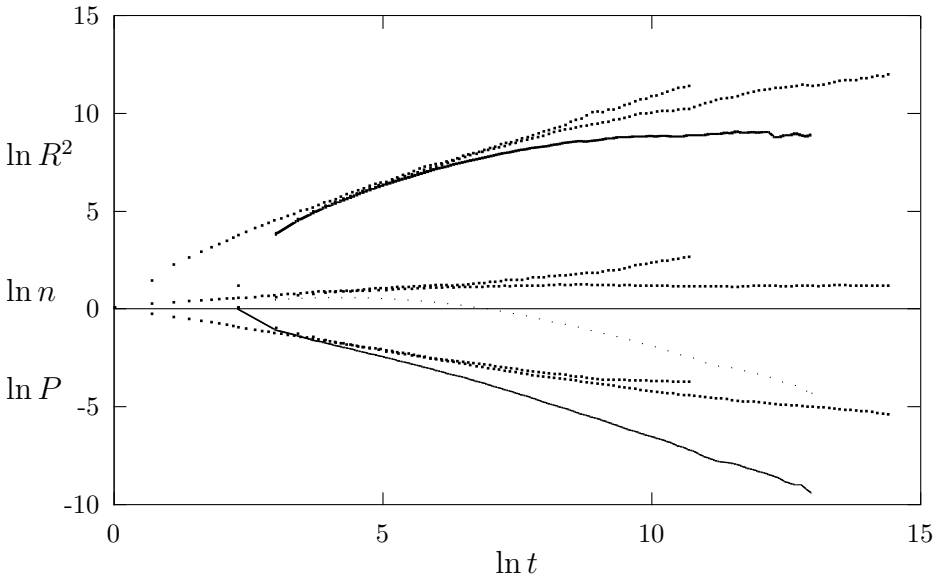


Figure 4.5: Plots of the survival probability $P(t)$, mean number of particles $n(t)$ and the mean-square distance of particles from the origin $R^2(t)$ versus $t$, in the diluted contact process for $x = 0.3$. In each plot, from bottom to top, we have $\lambda = 2.40; \lambda = 2.47$; and $\lambda = 2.50$.

may be given as follows (a more complete discussion is given in the next section). The probability of the seed landing in a favored region, of linear size $L$, in which the local density of diluted sites is such that $\lambda - \lambda_{c,eff} = \Delta$, is $\sim \exp(-AL^d)$. ($\lambda_{c,eff}$ is the critical creation rate for a system with the site density prevailing in this region.) The lifetime of the process in such a region is proportional to $\sim \exp(BL^d)$. (The precise forms of $A$ and $B$ are unknown, but it is clear that they are positive, increasing functions of $\Delta$ for $\Delta > 0$.) It follows that at long times

$$P(t) \sim max_{\Delta,L} \exp[-(AL^d + te^{-BL})] \sim max_{\Delta} t^{-A/B} \sim t^{-\phi}, \tag{4.12}$$

where the last step defines a (nonuniversal) decay exponent $\phi$. In fact, from Fig. (4.5), we see that this is the case for $\lambda = 2.40$ which is subcritical. In order to identify the critical curve we use the following criteria. It is known that the survival probability in the supercritical regime approaches a nonzero value, the ultimate survival probability $P_\infty$, at asymptotic times. Thus if $P(t)$ attains a plateau at later times, as for $\lambda = 2.50$ in Fig. (4.5), we know that this curve is supercritical. In order to refine this estimate, we observe that for $\lambda > \lambda_c$, $n(t)$ must grow monotonically at long times;

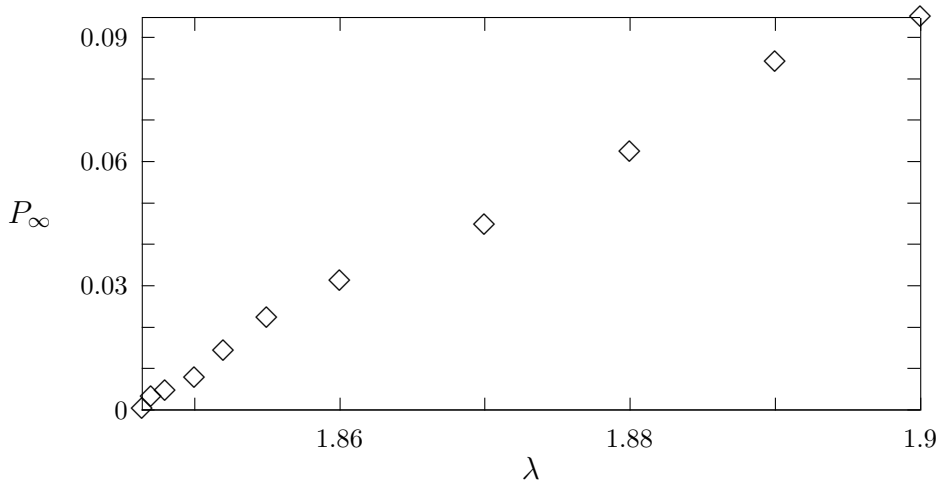


Figure 4.6: Plot of $P_\infty$ *versus* $\lambda$ for $x = 0.1$.

for $\lambda < \lambda_c$ it must decay. In the pure CP, for example, $n(t)$ grows for $\lambda \geq \lambda_c$, so $\lambda_c$ is the smallest $\lambda$ supporting asymptotic growth. In the present case we wish to stay clear of assumptions regarding the sign of $dn(t)/dt$ at critical; we simply note that growth (decay) rules out a particular $\lambda$ as being subcritical (supercritical). Using these conditions to winnow the set of possible critical values, we eventually find a narrow range of $\lambda$ for which $n(t)$ appears *steady* at long times. Based on these considerations we conclude that $\lambda_c(x = 0.3) = 2.47$.

Of note is the slow approach of $P(t)$ to its limiting value, $P_\infty$, in the supercritical regime, where we find that at long times $P(t) \approx P_\infty + const. \times t^{-y}$, with $y$ ranging from 1/2 (quite near critical) to 1 (at larger $\lambda$). In cases for which $P(t)$ has yet to attain its limit at $t_{max}$, we use expressions of this form to estimate $P_\infty$. Also evident in Fig. (4.5) is the power-law behavior in the subcritical, Griffiths phase.

We also studied the ultimate survival probability as a function of $\Delta$, for $\Delta > 0$. While $P_\infty$ and $\overline{\rho}_\bullet$ are described by the same exponent in the basic CP and other simple models, the same is not valid for models possessing multiple absorbing configurations [55]. $P_\infty$ is rather described by $P_\infty \sim \Delta^{\beta'}$, where $\beta'$ is the ultimate survival probability exponent. It is therefore a good idea to check if whether the exponents $\beta$ and $\beta'$ are equal. Fig. (4.6) shows $P_\infty$ versus $\lambda$ for $x = 0.1$; the data for other dilutions looks similar. We determined the ultimate survival probability exponent $\beta'$ for dilutions $x = 0.05; 0.1; 0.2; 0.3$ and 0.35. In Fig. (4.7) we show the log-log plots of $P_\infty$ versus $\Delta$ for some of these dilutions. Least-squares linear fits to plots of $\ln P_\infty$ versus $\ln(\lambda - \lambda_c)$,

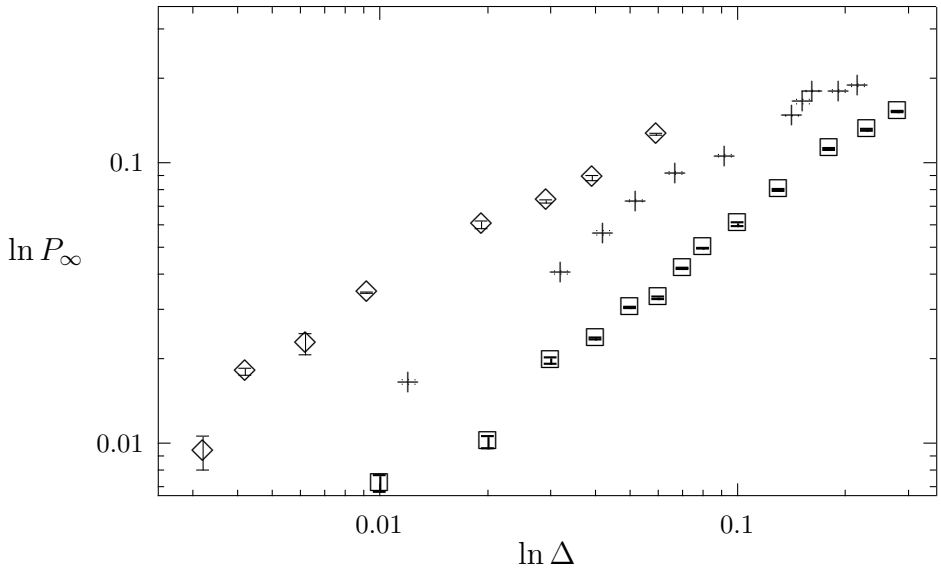


Figure 4.7: Logarithmic plot of the ultimate survival probability versus $\Delta = \lambda - \lambda_c(x)$ for dilutions $x = 0.05(\diamond), 0.2(+)$, and $0.35(\square)$, respectively.

as in Fig. (4.7), yield the estimates for $\beta'$ listed in Table 4.2. For $x \geq 0.05$ the $\beta'$ estimates cluster near unity; the mean is 0.99(3), not far from Noest's result, $\beta = 1.10(5)$ [57]. (Our preliminary results on the stationary density yield $\beta \simeq 1$ for $x = 0.35$.)

Having located the critical point $\lambda_c(x)$, we turn to the spreading behavior. Log-log plots of $P(t)$, and $R^2(t)$ at $\lambda_c$, as shown in Fig. (4.8), present substantial curvature at late times, prompting us to ask whether spreading is power-law or slower. The local slopes of these graphs, commonly employed to extract estimates for spreading exponents [8], here show all three exponents decreasing sharply at long times. By contrast, the same data approach linear asymptotes when plotted, as in Fig. (4.9), versus $\ln(\ln t)$. (Logarithmic decay of the survival probability has been observed in previous, less extensive simulations of the DCP [58].) For $x \geq 0.1$ expressions of the form $P(t) \sim (\ln t)^{-a}$ and $R^2(t) \sim (\ln t)^c$ fit the data over a larger range of times than do power laws. For $t \geq \tau_P(x)$, $P(t)$ is well-described by a logarithmic time-dependence; $\tau_P$ decreases from about 3500, for $x = 0.1$, to about 60 for $x = 0.35$. The approach of $R^2$ to a logarithmic growth law typically occurs earlier, at around $\tau_P/3$. For the weakest disorder studied ($x = 0.02$), we observe only (pure) DP-like spreading on the time scale of our simulations. The somewhat larger dilution of $x = 0.05$ presents an

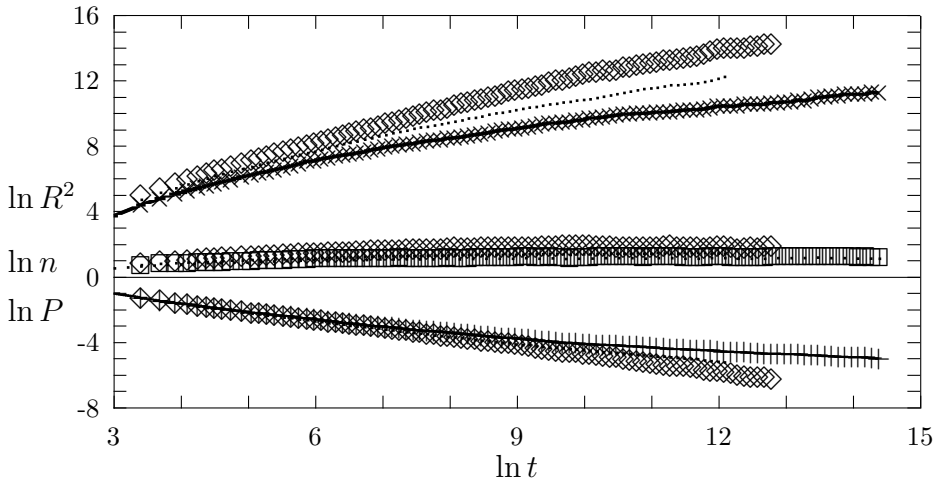


Figure 4.8: Log-log plots of the survival probability $P(t)$, mean number of particles $n(t)$ and the mean-square distance of particles from the origin $R^2(t)$ versus $t$, in the critical diluted contact process. $\diamond : x = 0.35, \lambda = 2.72$; dots:$x = 0.2, \lambda = 2.108$; full curve plus points : $x = 0.05, \lambda = 1.7408$.

intermediate case, in which the mean-square spread follows $R^2 \sim t^{1.18}$ for $t < 400$, and $R^2 \sim (\ln t)^c$ for $t > 1600$, but the survival probability is better described by a power law, $P \sim t^{-0.53}$, for $t < t_{max} = 4 \times 10^5$. (Note that the exponent estimates are fairly close to those of the pure CP.) For these small dilutions we expect a crossover to the logarithmic forms at larger $t$, but have been unable to verify this, due to computational limitations. The rapid decrease in $\tau_P$ with increasing dilution can be understood by noting that for weak disorder, the process must spread over a rather large area before randomness becomes manifest; for small $x$, sizable regions of the lattice look nearly regular.

Since our results for critical spreading are best characterized by logarithmic time-dependences, they are formally consistent with $\delta$, $\eta$, and $z$ all being zero. The powers $a$ and $c$ in the logarithmic fits for $P$ and $R^2$ vary systematically, and over a substantial range, as the dilution is varied (see Table 4.2). While we are confident that the critical exponent $\eta \simeq 0$, it is possible that $n(t) \sim (\ln t)^b$ with some small $|b|$. More precise determinations of $\lambda_c$ and/or of $n(t)$ at long times are required to resolve this question. The only previous determination of a spreading exponent we are aware of (for a model in this class), is Noest's result for the spreading dimension, $\hat{d} = 1.61(5)$ for disordered DP in 2+1 dimensions [57]. In our notation, $\hat{d} = 1 + \eta + \delta$,

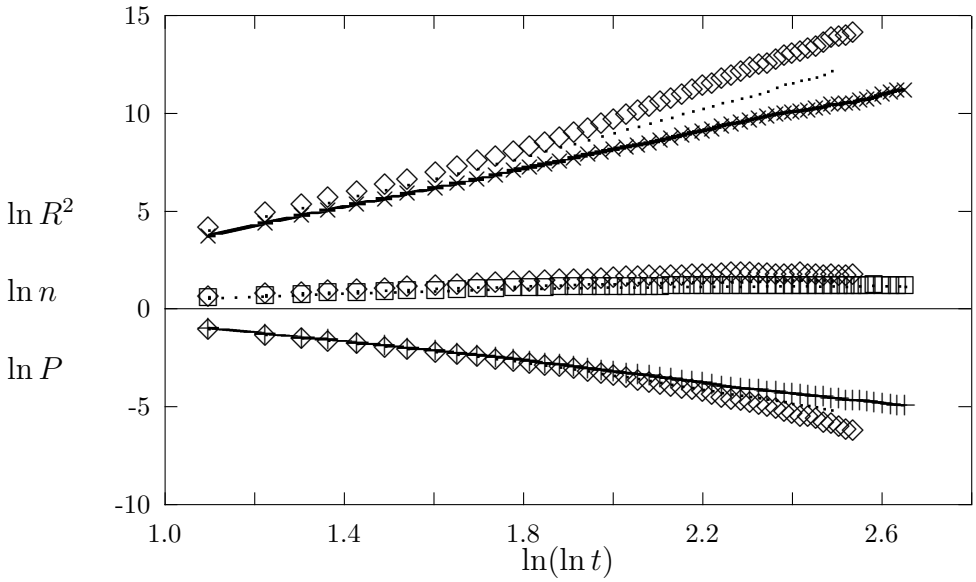


Figure 4.9: Plots of $\ln P(t)$, $\ln n(t)$ and $\ln R^2(t)$ versus $\ln(\ln t)$, in the critical diluted contact process. Full curve plus points: $x = 0.35, \lambda = 2.72$;dots:$x = 0.2, \lambda = 2.108$; $\diamond$ : $x = 0.05, \lambda = 1.7408$.

so our simulations yield $\hat{d} = 1$ (logarithmic spreading). (We obtain the same value if we extract the exponent directly from the data for $n(t)/P(t)$.) It is worth noting that our studies extend about 10 to 100 times longer in time (to at least $5 \times 10^4$, compared with $4 \times 10^3$ in Ref. [57]), and employ samples two to three orders of magnitude larger. The latter is of particular significance, since rare events appear to dominate the critical behavior in disordered systems.

As noted above, the decay of $P(t)$ should be governed by a power law in the range $\lambda_c(0) < \lambda < \lambda_c(x)$; examples of $P$, $n$, and $R^2$ in this regime are shown in Fig. (4.10). This plot confirms power-law decay, and shows that the exponents $\phi$ and $\zeta$ governing $P$ and $n$ ($\sim t^{\zeta}$) are nonuniversal in this regime, as expected [56, 58]. When $x = 0.35$, for example, we find $\phi \approx 2.2$ for $\lambda = 2.4$, and $\phi \approx 0.6$ for $\lambda = 2.65$; the corresponding values of $\zeta$ are -2.0 and -0.4. In all cases studied, however, the asymptotic growth (if any) of $R^2$ seems slower than power-law. (Prior to reaching a plateau, $R^2$ exhibits logarithmic growth.) Fig. 5 includes data for $x = 0.45$, i.e., a site concentration below the percolation threshold. In this regime power-law relaxation of $P(t)$ is expected for *any* $\lambda > \lambda_c(0)$.

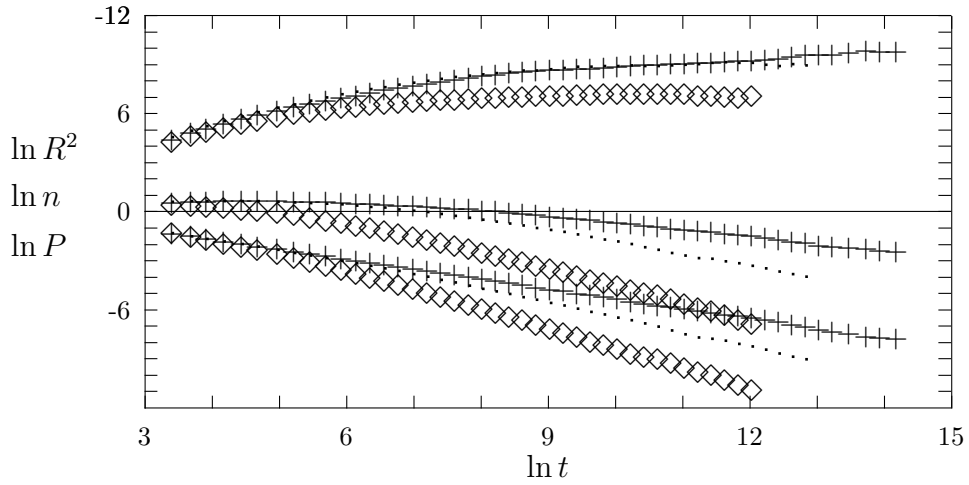


Figure 4.10: Logarithimic plots of the survival probability $P(t)$, mean number of particles $n(t)$ and the mean-square distance of particles from the origin $R^2(t)$ versus $t$, in the subcritical diluted contact process (Griffiths phase). $\diamond : x = 0.45, \lambda = 3.0; + : x = 0.35, \lambda = 2.65$; dots: $x = 0.3, \lambda = 2.40$.

## 4.5 Power-law Relaxation

In this section we review the power-law relaxation arguments devised by Noest [56]. Noest studied the effect of disorder on a stochastic cellular automaton (SCA) belonging to the DP universality class. In the SCA each site $i$ of a $d$-dimensional lattice can take either one of the two values $s_i \in \{0, 1\}$. The dynamics is given by the following transition rules

$$P(s_i(t+1) = 1) = F_i(\sum_j c_{ij} s_j(t)) \tag{4.13}$$

with $F_i(x = 0) = 0$ and $0 < F_i(x > 0) < 1$; and the $2d$ coupling $c_{ij} > 0$. The vacuum, $s_i = 0 \ \ \forall\, i$, is the unique absorbing state of the process. By setting $F(x > 0) = p$ and $c_{ij} = 1$ one recovers site directed percolation with site density $p$. It is important to remark that the contact process is a continuous-time version of the SCA [2].

For $d > 1$ spatial disorder is introduced in the form of random dilution: each site is either present with probability $p$, or absent with probability $1 - p$. Below the percolation threshold, $p^*$, a phase transition cannot take place. For $p > p^*$, the model has an active phase for a given $c_d^*$. Noest studied the two-dimensional SCA through Monte Carlo simulations for site dilutions 0; 0.05; 0.1; 0.2 and 0.3 [57]. In all cases, the

| | $p^* < p < 1$ | $p = 1$ | $(2+1)$-DP |
|---|---|---|---|
| $\delta + \eta$ | 0.61(5) | 0.81(4) | $0.674(14)^a$ |
| $\beta$ | 1.10(5) | 0.63(3) | $0.586(14)^b$ |
| $\nu_\perp$ | 1.17(10) | 0.84(5) | $0.729(8)^a$ |
| $\nu_\parallel$ | 2.0(15) | 1.3(1) | $1.286(5)^a$ |

Table 4.1: Critical exponents obtained through Monte Carlo simulations of the disordered SCA by Noest. The numbers in parenthesis indicate uncertainties. [a] Brower, Furman & Moshe, 1978; [b] Grassberger, 1989.

model was found to undergo a well-defined phase transition. The critical exponents of the disordered model were found to be quite different from the ones without disorder, which take the usual DP values. In Table 4.1 we report Noest's exponents for the pure and disordered two-dimensional SCA. From Table 4.2 we see that our results for $x = 0.3$ and 0.35 are incompatible with the ones obtained by Noest. It is important to remark that our results are concentrated on the two extremes of the dilution range and results for intermediate values may be necessary in order to draw further conclusions.

On the basis of a mechanism similar to the one responsible for the Griffiths phase in disordered spin models [59], a nonexponential decay to the vacuum state is expected in SCA models with quenched disorder. The basic physical mechanism underlying this power-law decay is simply the existence of large clusters in which the interactions are above the critical point, at which an infinite system can support an active phase. While the number of such clusters falls off exponentially with their size, their characteristic decay time grows exponentially. Noest derived lower and upper bounds with asymptotic power-law decay for site-diluted SCA models in dimensions $d \geq 1$.

It is easier to analyze the slow relaxation behavior for $p < p^*$, where no active phase can occur. The lower bounds derived are also applicable to $p > p^*$. The decay function $M(t) = \sum_n nP_nM_n(t)$ is defined as the fraction of sites with $s_i(t) = 1$ when starting from $s_i(0) = 1 \; \forall \; i$. $M_n(t) \sim \exp(-t/T_n)$ is the probability that an $n$ cluster has not yet reached the vacuum at time $t$, and $P_n$ is the probability of occurrence of an $n$-cell string. To find nonexponential asymptotic lower bounds for $M(t)$, one first considers the relaxation of compact, approximately spherical $n$-site clusters. Note that the asymptotics of $M(t)$ are the same as those of the survival probability, $P(t)$, when starting from a configuration with a single seed at the origin. The long-time

behavior of $M(t)$ is dominated by rare compact clusters with favorable fluctuations in the density of non-diluted sites. In a spreading simulation, there is a finite probability of the seed landing in such a cluster, and a finite probability that the process spreads to fill this cluster at a finite density, since the cluster is "supercritical". The density of non-diluted sites in this cluster is such that the critical parameter for this density is below the parameter considered critical for the diluted system. Once these two events occur — landing in the favorable cluster, and surviving there — the decay of $P(t)$ will be just like the decay of $M(t)$. So, focusing on this specific cluster, one would expect that at long times $P(t) \sim cM(t)$, where $c$ is a constant smaller than 1 as not all trials survive. The important point is that $P(t)$ and $M(t)$ have the same lifetime.

The SCA model decays to the vacuum on a time scale growing as

$$T_n \sim \exp(an) \tag{4.14}$$

for $c > c_d^*$, where $a$ is a constant. The exponential growth is expected because a locally supercritical cluster decays only through coherent fluctuations involving all its sites. Such compact clusters occur with probability

$$\ln P_n = -bn - b'm + \mathcal{O}(\ln n) \tag{4.15}$$

where $b \sim -\ln p, b' \sim -\ln(1-p)$, and $m = n^{(d-1)/d}$. The three factors in $P_n$ come from contributions of the (dense) bulk, the (empty) outer surface and the multiplicity of cluster shapes with the same $T_n$. The long-tailed relaxation of these dense clusters gives a lower bound $M'(t)$ for $M(t)$,

$$M'(t) = \sum_n nP_n \exp(-t/T_n) \sim \int_0^\infty dn\ n \exp[-bn - t\exp(-an) - b'n^{(d-1)/d}] \tag{4.16}$$

where by replacing the sum by the integral one can use the Laplace's method to find the large-$t$ behavior. One finds the asymptotic forms determined by the maximum of the square bracket occurring at $n = (1/a)\ln(at/b) + \mathcal{O}[(\ln t)^{-1/d}]$. This yields

$$\ln M'(t) \sim -\frac{b}{a}\ln(\frac{at}{b}) + [\frac{1}{a}\ln(\frac{at}{b})]^{(d-1)/d}. \tag{4.17}$$

The dominant contribution to $M'(t)$ is the power-law term with exponent $-b/a$.

One can also construct a power-law upper bound $M''(t)$. The idea is to count all the clusters, instead of just the compact ones, and to use the decay time of the slowest $n$ cluster as upper bound for the decay time of the unrestricted $n$ clusters. For any $p < p^*$, the number density of $n$-site clusters decreases exponentially for large $n$.

| $x$ | $\lambda_c$ | $\beta'$ | $a$ | $c$ |
|---|---|---|---|---|
| 0 | 1.6488(1) | 0.586(14) | — | — |
| 0.02 | 1.6850(3) | 0.566(7) | — | — |
| 0.05 | 1.7409(1) | 0.97(10) | — | 8.6(3) |
| 0.1 | 1.84640(5) | 0.89(4) | 4.6(1) | 8.1(1) |
| 0.2 | 2.1080(5) | 0.99(4) | 3.64(14) | 6.3(2) |
| 0.3 | 2.470(3) | 1.07(3) | 3.05(15) | 5.30(6) |
| 0.35 | 2.719(2) | 1.01(5) | 2.72(5) | 4.78(5) |

Table 4.2: Critical parameters from simulations of the DCP. Numbers in parentheses indicate uncertainties.

Thus $\ln P_n \sim -b''n$ with $0 < b'' < b$. The decay time of any $n$-site cluster is bounded above by the usual $T_n \sim \exp(an)$ of a compact cluster of the same mass. Hence,

$$M''(t) \sim \int_0^\infty dn\ n \exp[-b''n - t\exp(-an)] \tag{4.18}$$

leading to the power-law upper bound $M''(t) \sim t^{-b''/a}$ where $0 < b'' \leq b$ for all $c > c^*$ and $p < p^*$. Thus the asymptotic decay of $M(t)$ is also a power law.

## 4.6 Summary

In Table 4.2 we list the critical parameters, the exponent $\beta'$ and the parameters $a$ and $c$ of the logarithmic behavior we found for the diluted contact process. The data in this table confirm that $\lambda_c$ depends on dilution approximately as $\lambda_c(x) \approx \lambda_c(0)/(1-x)$, as predicted by our mean-field results. Dilution inhibits creation by reducing the effective number of neighbors, thus it is natural that the critical creation rate grows with $x$.

For the smallest dilution studied ($x = 0.02$) there is no evidence of a change in the growth-law on simulation time scales. Hence the critical exponents for $x = 0.02$ are in a pretty good agreement with the exponents for $x = 0$ (pure CP). Based on our results for dilutions $x = 0.05; 0.1; 0.2; 0.3$ and 0.35 we see that quenched disorder has a dramatic effect on the critical behavior of the contact process. For the critical DCP, the survival probability and the mean-square distance from the origin show a logarithmic dependence on time. Also, the population size is characterized by a

totally new behavior. In the pure critical CP $n(t)$ increases monotonically with time; $\eta$ in eq. (4.5) is positive. In the critical DCP $n(t)$ is constant at long times, $\eta$ is *zero*.

Noest's simulations of the one- and two-dimensional disordered stochastic cellular automaton (SCA) yielded critical exponents quite different from the usual DP exponents, suggesting a new universality class characterizing disordered directed percolation. A related field-theoretic study by Obukhov [60] yielded results qualitatively consistent with the large values of the critical indices found by Noest. As argued by Noest [56] the survival probability may have a power-law decay rather than an exponential decay (as expected in pure systems), in a phenomenon similar to that in Griffiths phase.

Bramson, Durrett and Schonmann studied a one-dimensional CP with disorder in the form of a death rate randomly taking one of two values (independently) at each site [61]. They demonstrated that this model possesses an intermediate phase in which survival (starting, e.g., from a single particle) is possible, but the active region grows more slowly than linearly; sub-linear growth has also been observed in simulations [62]. (In the pure CP the radius of the active region grows $\propto t$ for any $\lambda > \lambda_c$.) In two or more dimensions, Bramson et al. conjectured, there is no intermediate phase. Our results for various dilutions support this conjecture. For example, simulations at $x = 0.1$, with $\lambda$ close to, but slightly above $\lambda_c$ (to be precise, $\lambda = 1.86$ and 1.87, corresponding to $(\lambda - \lambda_c)/\lambda_c = 0.007$ and 0.013, respectively), showed $n(t) \sim t^2$ (and similarly for $R^2(t)$), consistent with the radius of the active region growing $\sim t$. Thus a sublinear-growth phase, if it exists at all, is confined to a very narrow range of creation rates. While our model incorporates dilution rather than a random death rate, one would expect such an intermediate phase to be a rather general feature of disordered contact processes, so that its apparent absence here argues for the validity of the conjecture.

In summary, we find that quenched disorder induces a radical change in the critical spreading of the contact process. In contrast to the well-known power laws in the pure CP, we observe logarithmic time-dependence. Although our results are restricted to dilutions $0.05 \leq x \leq 0.35$, we expect a crossover to logarithmic behavior for all $0 < x < 1 - p_c$, albeit at very long times for small $x$. While we are inclined to suppose that the DCP is but one member of a universality class encompassing all disordered models with a continuous transition to a unique absorbing configuration, studies of absorbing-state transitions in other disordered models are needed to verify the universality hypothesis.

# Chapter 5

# Series Expansions in Pair-contact Process

## 5.1 Introduction

Series expansions have been successfully applied to nonequilibrium systems exhibiting a continuous transition to an absorbing state [14, 27, 29, 30]. They have become very efficient tools for calculating critical parameters, and also provide information about off-critical behavior. In steady-state series expansions [14, 27] one expands about a model whose time dependence may be solved exactly. This provides a formalism which may then be implemented for a particular model, as represented by its evolution operator. In time-dependent series expansions [29, 30] one derives, starting from the master equation, a perturbative expansion for the long- and short-time behavior of quantities such as the survival probability and the mean number of particles, when evolving from a single seed initial state.

In this chapter we develop a time-dependent series expansion formalism and describe its application to the one-dimensional pair-contact process (PCP) model. The chapter is organized as follows. In the next section we introduce the model. An operator formalism for the master equation is presented in section (5.3). In section (5.4) we derive the time-dependent perturbation theory. An illustration of the method is presented in section (5.5). In section (5.6) we show how to implement an algorithm to generate the series terms. In section (5.7) we present and discuss the results.

## 5.2 The model

The pair-contact process is a simple one-component model in which pairs – two nearest neighbor occupied sites – are annihilated with probability $p$, while with probability $1-p$, a new particle is created at a vacant nearest neighbor of the pair. Fig. (5.1) illustrates the rules of the process.

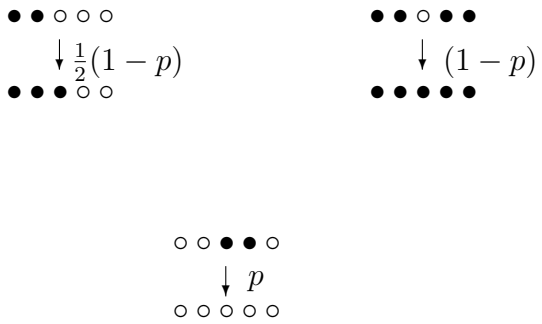


Figure 5.1: Diagram showing the rules for the one-dimensional pair-contact process. The top represents two possible configurations of a creation event, and the bottom a pair annihilation event.

The order parameter of the model is the concentration of pairs. The absence of pairs characterizes the absorbing state. The PCP exhibits a continuous transition between an active and an absorbing state as $p$ is increased beyond $p_c = 0.0771$ [39, 40]. The phase diagram of the model is shown in Fig. (5.2).

While the absorbing state is unique in the sense of its having a complete absence of pairs, from the particle point of view there are many such states, which makes the PCP a model with multiple absorbing configurations. Such models show anomalous behavior [40, 66]. In particular, the time-dependent exponents ($\eta, \delta$ and $z$, pertinent to spreading from an initial state close to an absorbing state [22]) of the PCP show a dependence on the initial configuration, as it allows a vast choice of initial states. For natural initial configurations (those generated by the dynamics of the system), the time-dependent exponents take their usual DP values. For that matter, static exponents such as $\beta, \nu_{\parallel}$ and $\nu_{\perp}$ also assume DP values [40].

The results discussed above were obtained through simulations. Our aim is to get more insight into the time-dependent behavior of the PCP using series expansions.

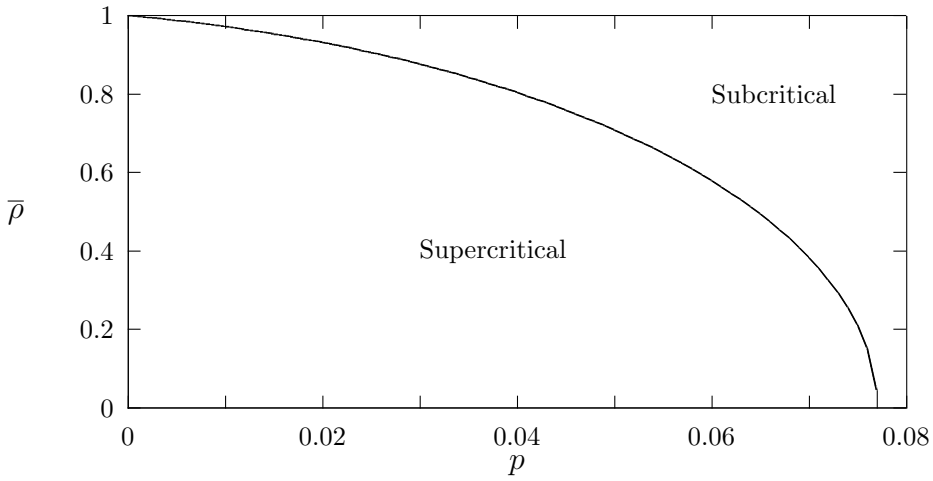


Figure 5.2: Steady-state concentration of pairs as a function of the pair annihilation probability. For $p < p_c$ the system is in the supercritical region, and for $p > p_c$ the system is in the subcritical region.

## 5.3 Operator Formalism

Markov processes in many-particle systems may be conveniently described via an operator formalism. In this work we use the formalism of references [14] and [30], in which only single occupancy of sites is allowed. A more complete description of this formalism can be found in [63, 64, 65].

The basis states of a given site $i \in Z^d$ are represented by $|\phi_{\sigma_i,i}\rangle$ where $\sigma_i = 0, 1$ stands for a vacant or occupied site, respectively. Any configuration $\{\sigma_i\}$ of the system can be written as a direct product

$$|\{\sigma_i\}\rangle = \prod_{i \in Z^d} |\phi_{\sigma_i,i}\rangle. \tag{5.1}$$

The inner product is given by

$$\langle\{\sigma_i\}|\{\sigma_i'\}\rangle = \prod_{i \in Z^d} \delta_{\sigma_i,\sigma_i'}. \tag{5.2}$$

Creation and annihilation operators for site $i$ are defined as

$$A_i^\dagger |\phi_{\sigma_i,i}\rangle = (1 - \sigma_i)|\phi_{1-\sigma_i,i}\rangle \tag{5.3}$$

$$A_i |\phi_{\sigma_i,i}\rangle = \sigma_i |\phi_{1-\sigma_i,i}\rangle \tag{5.4}$$

which obey the relation $A_i A_i^\dagger + A_i^\dagger A_i = 1$. The state of a system at time $t$ is represented by

$$|\Psi(t)\rangle = \sum_{\{\sigma_i\}} p(\{\sigma_i\}, t)\ |\{\sigma_i\}\rangle, \tag{5.5}$$

where we are summing over all configurations and $p(\{\sigma_i\}, t)$ is the probability distribution on configuration space. Only states satisfying positivity and normalization are physically relevant. These conditions are expressed by

$$\langle\{\sigma_i\}|\Psi\rangle \ \geq \ 0, \quad \forall\ \{\sigma_i\} \tag{5.6}$$

$$\sum_{\{\sigma_i\}} \langle\{\sigma_i\}|\Psi\rangle \ = \ 1. \tag{5.7}$$

The evolution of the probability distribution is governed by the master equation,

$$\frac{d|\Psi(t)\rangle}{dt} = S|\Psi(t)\rangle \tag{5.8}$$

whose formal solution (given that $S$ is time independent) is

$$|\Psi(t)\rangle = e^{St}|\Psi(0)\rangle \tag{5.9}$$

where $|\Psi(0)\rangle$ is the initial probability distribution.

The master equation for the pair-contact process is given by

$$\begin{aligned}\frac{dp(\{\sigma\}, t)}{dt} = &- \sum_{\{\sigma\}'} \ w(\{\sigma\} \to \{\sigma\}') \ \ p(\{\sigma\}, t) + \sum_{\{\sigma\}'} w(\{\sigma\}' \to \{\sigma\}) p(\{\sigma\}', t) \\ &- \sum_{\{\sigma\}''} \ w(\{\sigma\} \to \{\sigma\}'') \ \ p(\{\sigma\}, t) + \sum_{\{\sigma\}''} w(\{\sigma\}'' \to \{\sigma\}) p(\{\sigma\}'', t)\end{aligned} \tag{5.10}$$

where we have taken out the indices for simplicity, and

$$|\{\sigma\}'\rangle_j = |\phi_{1-\sigma_j, j}\rangle \prod_{i(i\neq j)} |\phi_{\sigma_i, i}\rangle$$

denotes a configuration identical to $|\{\sigma\}\rangle = \prod_i |\phi_{\sigma_i, i}\rangle$ except for the site $j$. In the same way,

$$|\{\sigma\}''\rangle_j = |\phi_{1-\sigma_j, j}\rangle |\phi_{1-\sigma_{j+1}, j+1}\rangle \prod_{i(i\neq j, j+1)} |\phi_{\sigma_i, i}\rangle$$

denotes a configuration identical to $|\{\sigma\}\rangle = \prod_i |\phi_{\sigma_i,i}\rangle$, except by the pair situated at $(j, j+1)$. The master equation is constructed as follows: each term is formed by the product of the probability of being in a particular configuration and the transition rate of going from this configuration to another one. For example, the first term expresses a situation in which the system is in configuration $|\{\sigma\}\rangle$ at time $t$ and suffers a transition to $|\{\sigma\}'\rangle$ as a particle is created at site $j$. As this term decreases the probability $p(\{\sigma\}, t)$ it carries a minus sign. The other terms are obtained analogously. By multiplying both sides of the master equation by $|\{\sigma\}\rangle$ and summing over $\{\sigma\}$ we get

$$\begin{aligned}\frac{d|\Psi(t)\rangle}{dt} = & - \sum_{\{\sigma\}\{\sigma\}'} w(\{\sigma\} \to \{\sigma\}')p(\{\sigma\}, t)|\{\sigma\}\rangle \\ & + \sum_{\{\sigma\}\{\sigma\}'} w(\{\sigma\}' \to \{\sigma\})p(\{\sigma\}', t)|\{\sigma\}\rangle \\ & - \sum_{\{\sigma\}\{\sigma\}''} w(\{\sigma\} \to \{\sigma\}'')p(\{\sigma\}, t)|\{\sigma\}\rangle \\ & + \sum_{\{\sigma\}\{\sigma\}''} w(\{\sigma\}'' \to \{\sigma\})p(\{\sigma\}'', t)|\{\sigma\}\rangle.\end{aligned} \tag{5.11}$$

As we are summing over $\{\sigma\}$ and $\{\sigma\}'$ or $\{\sigma\}$ and $\{\sigma\}''$ we may interchange $\{\sigma\}$ and $\{\sigma\}'$ and $\{\sigma\}$ and $\{\sigma\}''$ in the positive rhs terms to get

$$\begin{aligned}\frac{d|\Psi(t)\rangle}{dt} = & - \sum_{\{\sigma\}\{\sigma\}'} w(\{\sigma\} \to \{\sigma\}')p(\{\sigma\}, t)|\{\sigma\}\rangle \\ & + \sum_{\{\sigma\}\{\sigma\}'} w(\{\sigma\} \to \{\sigma\}')p(\{\sigma\}, t)|\{\sigma\}'\rangle \\ & - \sum_{\{\sigma\}\{\sigma\}''} w(\{\sigma\} \to \{\sigma\}'')p(\{\sigma\}, t)|\{\sigma\}\rangle \\ & + \sum_{\{\sigma\}\{\sigma\}''} w(\{\sigma\} \to \{\sigma\}'')p(\{\sigma\}, t)|\{\sigma\}''\rangle.\end{aligned} \tag{5.12}$$

The transition rate $w(\{\sigma\} \to \{\sigma\}'')$, related to the annihilation of one pair, is proportional to the probability $p$,

$$w(\{\sigma\} \to \{\sigma\}'') = p\sigma_i\sigma_{i+1}, \tag{5.13}$$

where the product $\sigma_i\sigma_{i+1}$ is different from zero when sites $i$ and $i+1$ are occupied and zero otherwise. The transition rate $w(\{\sigma\} \to \{\sigma\}')$, related to the creation of one

particle is given by

$$w(\{\sigma\} \to \{\sigma\}') = \frac{1}{2}(1-p)(1-\sigma_i)(\sigma_{i-2}\sigma_{i-1} + \sigma_{i+1}\sigma_{i+2}), \tag{5.14}$$

where $(1-\sigma_i)$ assures that site $i$ is vacant, and $(\sigma_{i-2}\sigma_{i-1}+\sigma_{i+1}\sigma_{i+2})$ equals two if site $i$ has two nearest neighbor pairs, one if site $i$ has only one nearest neighbor pair and zero if none. Substituting these rates in the master equation we have,

$$\begin{aligned}\frac{d|\Psi(t)\rangle}{dt} &= -\frac{1}{2}(1-p)\sum_{\{\sigma\}}\sum_i(1-\sigma_i)(\sigma_{i-2}\sigma_{i-1}+\sigma_{i+1}\sigma_{i+2})(|\{\sigma\}\rangle - |\{\sigma\}'\rangle)p(\{\sigma\},t) \\ &- p\sum_{\{\sigma\}}\sum_i \sigma_i\sigma_{i+1}(|\{\sigma\}\rangle - |\{\sigma\}''\rangle)p(\{\sigma\},t).\end{aligned} \tag{5.15}$$

Using the expressions for $A$ and $A^\dagger$, eqs. (5.3) and (5.4), the master equation becomes

$$\frac{d|\Psi(t)\rangle}{dt} = -p\sum_i(A_i^\dagger A_i A_{i+1}^\dagger A_{i+1} - A_iA_{i+1})|\Psi(t)\rangle$$

$$+\frac{1}{2}(1-p)\sum_i[(1-A_i)A_i^\dagger][A_{i-1}^\dagger A_{i-1}A_{i-2}^\dagger A_{i-2} + A_{i+1}^\dagger A_{i+1}A_{i+2}^\dagger A_{i+2}]|\Psi(t)\rangle. \tag{5.16}$$

By writing eq. (5.16) in the form of eq. (5.8) we find that the evolution operator $S$ for the pair-contact process takes the form

$$\begin{aligned}S = &+ \frac{1}{2}(1-p)\sum_i[(1-A_i)A_i^\dagger][A_{i-1}^\dagger A_{i-1}A_{i-2}^\dagger A_{i-2} + A_{i+1}^\dagger A_{i+1}A_{i+2}^\dagger A_{i+2}] \\ &- p\sum_i(A_i^\dagger A_i A_{i+1}^\dagger A_{i+1} - A_iA_{i+1}),\end{aligned} \tag{5.17}$$

which can be rewritten as,

$$S = \lambda W + V \tag{5.18}$$

where

$$W = \sum_{i\in Z^d}(A_iA_{i+1} - A_i^\dagger A_i A_{i+1}^\dagger A_{i+1}), \tag{5.19}$$

$$V = \frac{1}{2}\sum_{i\in Z^d}(1-A_i)A_i^\dagger(A_{i-1}^\dagger A_{i-1}A_{i-2}^\dagger A_{i-2} + A_{i+1}^\dagger A_{i+1}A_{i+2}^\dagger A_{i+2}), \tag{5.20}$$

and

$$\lambda = \frac{p}{(1-p)}, \tag{5.21}$$

where a $(1-p)^{-1}$ factor is absorbed into a rescaling of the time variable in eq. (5.8). In this decomposition $W$ only annihilates pairs and $V$ only creates particles.

The next step is to consider the effects of the operators $W$ and $V$ on any configuration. Operating with $W$ on a configuration $(C)$, where $(C)$ contains $r$ pairs, it gives a sum of $r$ configurations $(C')$ (each having one of the $r$ pairs vacated), minus $r$ times $(C)$ itself:

$$W(C) = \sum_{i=1}^{r}(C_i') - r(C) \tag{5.22}$$

Operating with $V$ on a configuration $(C)$ in which there are $q$ vacant sites nearest neighbors of at least one pair yields

$$V(C) = \sum_{i=1}^{q} f_i[(C_i'') - (C)], \tag{5.23}$$

where $f_i = \frac{1}{2}$ or 1, if a vacant site has one or two nearest neighbor pairs, respectively. $(C'')$ corresponds to the configuration $(C)$ with one of the $q$ vacant sites occupied. Notice that both $W$ and $V$ annihilate the absorbing state.

## 5.4 Time-dependent Perturbation Theory

In this section we develop a perturbative expansion for the time-dependent probability distribution, $|\Psi(t)\rangle$, for the one-dimensional pair-contact process. There are several ways of expanding eq. (5.9), for example, in terms of $t$ (short-time expansions), in terms of $\lambda$, or in terms of $\mu = \lambda^{-1}$. The expansion in powers of $t$ is obtained by chosing a value for $\lambda$ (the obvious choice being $\lambda_c$) and then truncating the series at some order $n$:

$$|\Psi(t)\rangle \approx \sum_{j=0}^{n} \frac{t^j}{j!}|\Psi_j\rangle, \tag{5.24}$$

where $|\Psi_j\rangle = S^j|\Psi(0)\rangle$. Considering the initial distribution $|\chi_0\rangle$, which attributes unit probability to the configuration that has one pair at the origin and all other sites vacant, we get the following recursive relation for $|\Psi_j\rangle$:

$$\begin{aligned} |\Psi_0\rangle &= |\chi_0\rangle \\ |\Psi_j\rangle &= (\lambda W + V)|\Psi_{j-1}\rangle; \qquad j \geq 1. \end{aligned} \tag{5.25}$$

As we operate with $V$ once in each step, the state $|\Psi_j\rangle$ is a sum over configurations containing up to $j+2$ particles. The coefficient of $t^j$ in the series for $n(t)$ is obtained by summing the products of the coefficient and the number of particles in each configuration. The coefficients in the expansion for $P(t)$ could be obtained simply by summing all the coefficients of the nonabsorbing configurations in $|\Psi_j\rangle$. It is, however, much simpler to calculate the extinction probability $p(t)$, the probability of having entered the absorbing state, which is related to $P(t)$ through the relation $P(t) = 1 - p(t)$. The coefficient of $t^j$ in the expansion of $p(t)$ is simply the coefficient of the absorbing configurations in $|\Psi_j\rangle$, i.e., configurations without pairs.

In order to derive an expansion in powers of $\lambda$ for the ultimate survival probability $P_\infty$, we consider the long-time behavior in the supercritical regime. In this expansion we treat the annihilation operator $W$ as a perturbation. The unperturbed evolution never reaches the absorbing state, so for small $\lambda$ we are clearly in the supercritical region. We expect the critical point to be associated with the first singularity on the positive $\lambda$ axis. Considering the Laplace transform of $|\Psi(t)\rangle$,

$$|\tilde{\Psi}(s)\rangle = \int_0^\infty dt\; e^{-st}|\Psi(t)\rangle = (s - S)^{-1}|\Psi(0)\rangle, \tag{5.26}$$

assuming that $|\tilde{\Psi}(s)\rangle$ can be expanded in powers of $\lambda$,

$$|\tilde{\Psi}(s)\rangle = |\tilde{\Psi}_0\rangle + \lambda|\tilde{\Psi}_1\rangle + \lambda^2|\tilde{\Psi}_2\rangle + \cdots, \tag{5.27}$$

and inserting eqs. (5.27) and (5.18) in eq. (5.26), we find

$$|\tilde{\Psi}_0\rangle \;=\; (s - V)^{-1}|\chi_0\rangle, \tag{5.28}$$

$$|\tilde{\Psi}_n\rangle \;=\; (s - V)^{-1}W|\tilde{\Psi}_{n-1}\rangle; \qquad n \geq 1. \tag{5.29}$$

The effect of $(s - V)^{-1}$ on a configuration $(C)$ can be found using eq. (5.23) and the identity (valid for any configuration)

$$(s - V)^{-1}(C) = s^{-1}(C) + s^{-1}(s - V)^{-1}\, V(C), \tag{5.30}$$

which together yield

$$(s - V)^{-1}(C) = (s + \sum_{i=1}^{q} f_i)^{-1}[(C) + (s - V)^{-1} \sum_{i=1}^{q} f_i(C_i'')], \tag{5.31}$$

where $q$ is the number of vacant sites nearest neighbor of at least one pair. As $V$ only creates configurations having one additional particle, it is clear that applying

$(s-V)^{-1}$ to any configuration, except the absorbing ones, we generate a infinite set of configurations. Therefore, it becomes impossible to compute $|\tilde{\Psi}(s)\rangle$ completely. On the other hand, we can easily calculate the extinction probability $\tilde{p}(s)$. The coefficient of $\lambda^j$ in the expansion of $\tilde{p}(s)$ is the sum of the coefficient of the absorbing configurations in $|\tilde{\Psi}_j\rangle$. The ultimate survival probability $P_\infty$ is then given by $P_\infty = 1 - \lim_{s\to 0} s\tilde{p}(s)$.

We will now consider the long-time behavior in the subcritical region. We treat $V$ perturbatively, instead of $W$, and expand $|\Psi(t)\rangle$ in terms of $\mu = \lambda^{-1}$. We rewrite $S$ as

$$S = W + \mu V, \tag{5.32}$$

where a factor $\lambda$ is absorbed into a rescaling of the time variable in eq. (5.8). The unperturbed evolution operator $e^{Wt}$ corresponds to an exponentially decaying chance of survival. Thus in the infinite-time limit only the absorbing states remain, and we are studying the subcritical regime. By taking the Laplace transform of eq. (5.9) and assuming that $|\tilde{\Psi}(s)\rangle$ can be expanded in powers of $\mu$, we obtain

$$|\tilde{\Psi}(s)\rangle = |\tilde{\Psi}_0\rangle + \mu|\tilde{\Psi}_1\rangle + \mu^2|\tilde{\Psi}_2\rangle + \cdots, \tag{5.33}$$

In analogy to eqs. (5.28) and (5.29), we have

$$|\tilde{\Psi}_0\rangle = (s-W)^{-1}|\chi_0\rangle, \tag{5.34}$$

$$|\tilde{\Psi}_n\rangle = (s-W)^{-1}V|\tilde{\Psi}_{n-1}\rangle; \qquad n \geq 1. \tag{5.35}$$

An identity equivalent to that obtained for eq. (5.30) also holds for $(s-W)^{-1}$, which together with eq. (5.22) yields,

$$(s-W)^{-1}(C) = (s+r)^{-1}[(C) + (s-W)^{-1}\sum_{i=1}^{r}(C_i')], \tag{5.36}$$

where $r$ is the number of pairs in configuration $(C)$. The coefficient of $\mu^j$ in the expansion for the survival probability $\tilde{P}(0)$, is the sum of the coefficients of all configurations, except the absorbing ones, in $|\tilde{\Psi}_j\rangle$. The corresponding coefficient in the expansion for the mean number of particles $\tilde{n}(0)$, is the sum of the product of the coefficient and the number of particles for each configuration.

## 5.5 A few terms for the one-dimensional PCP

In this section we derive a few terms for the critical time, supercritical and subcritical series as an illustration of the method described in the preceding sections. We denote an occupied site by $\bullet$ and a vacant site by $\circ$. Since time-dependent analysis focuses on the evolution of a system starting from a configuration close to the absorbing state (a single pair at the origin), we will deal with configurations in which most of the sites are vacant. For example, the initial configuration $|\chi_0\rangle$, which assigns probability 1 to the configuration with a single pair and all other sites vacant, is denoted by $(\bullet\bullet) = \sum_i A_i^\dagger A_{i+1}^\dagger|0\rangle$. In the same way, $(\bullet \circ \bullet) = \sum_i A_i^\dagger A_{i+2}^\dagger|0\rangle$ has two occupied sites separated by a vacancy, and so on. The translational invariance of the model is implicit in this notation.

**Supercritical Expansions**

We compute the extinction probability, in the supercritical regime, for the one- dimensional PCP to $\mathrm{O}(\lambda^1)$. By applying eqs. (5.28) and (5.29) to the initial configuration, $|\chi_0\rangle = (\bullet\bullet)$, we have

$$|\tilde{\Psi}_0\rangle = (s - V)^{-1}(\bullet\bullet).$$

In this case, we have $q = 2$ and $f_1 = f_2 = \frac{1}{2}$, as each vacant site has only one nearest neighbor pair. Thus,

$$(s - V)^{-1}(\bullet\bullet) = (s + 1)^{-1}(\bullet\bullet) + (s + 1)^{-1}(s - V)^{-1}(\bullet\,\bullet\,\bullet) + \cdots.$$

The generation of the subsequent terms follows the same reasoning, yielding

$$|\tilde{\Psi}_0\rangle = (s + 1)^{-1}(\bullet\bullet) + (s + 1)^{-2}(\bullet\,\bullet\,\bullet) + (s + 1)^{-3}(\bullet\,\bullet\,\bullet\bullet) + \cdots. \tag{5.37}$$

Notice that we discard all configurations with more than 3 pairs, as they do not contribute to the extinction probability at this order. To get $|\tilde{\Psi}_1\rangle$ we first apply $W$ to $|\tilde{\Psi}_0\rangle$,

$$\begin{aligned} W|\tilde{\Psi}_0\rangle = (s + 1)^{-1}[(0) \;&-\; (\bullet\bullet)] + 2(s + 1)^{-2}[(\bullet) - (\bullet\,\bullet\,\bullet)] \\ &+\; (s + 1)^{-3}[2(\bullet\bullet) + (\bullet \circ \circ\bullet) - 3(\bullet\,\bullet\,\bullet\bullet)]. \end{aligned} \tag{5.38}$$

As we are looking for the extinction probability, and the operator $(s - V)^{-1}$ only creates particles, we do not need to go further and compute $|\tilde{\Psi}_1\rangle$ completely. Note that by applying $(s - V)^{-1}$ over absorbing configurations they will be multiplied by

a factor $s^{-1}$, as $q = 0$ for these configurations. All other configurations carry one or more $(s + \sum_i f_i)^{-1}$ factors, corresponding to an eventual exponential decay in the survival probability. By collecting the coefficients of the absorbing configurations in eq. (5.38) we get the ultimate survival probability $P_\infty$, to $\mathrm{O}(\lambda^1)$,

$$\begin{aligned} P_\infty &= 1 - \lim_{s\to 0} s\tilde{p}(s), \\ P_\infty &= 1 - 4\lambda + \cdots . \end{aligned} \tag{5.39}$$

**Subcritical Expansions**

We calculate now the subcritical expansions for $\tilde{P}(0)$ and $\tilde{n}(0)$ to $\mathrm{O}(\mu^2)$. In order to simplify the notation, we will replace $(s+r)^{-1}$ by $r^{-1}$, as we are interested in the series only in the limit of $s \to 0$. Starting from the initial configuration $|\chi_0\rangle = (\bullet\bullet)$, $|\tilde{\Psi}_0\rangle$ is obtained by applying the operator $(s - W)^{-1}$ on $|\chi_0\rangle$

$$\begin{aligned} |\tilde{\Psi}_0\rangle &= (s - W)^{-1}(\bullet\bullet), \\ |\tilde{\Psi}_0\rangle &= (\bullet\bullet) + (0). \end{aligned}$$

At this point, we can discard the absorbing configurations at $|\tilde{\Psi}_0\rangle$, as they will be annihilated by applying $V$. According to eq. (5.35) the other terms are generated by operating with $(s - W)^{-1}V$ over $|\tilde{\Psi}_0\rangle$, and so on. Thus we find

$$\begin{aligned} |\tilde{\Psi}_1\rangle &= (s - W)^{-1}[(\bullet\,\bullet\,\bullet) - (\bullet\bullet)] = \frac{1}{2}(\bullet\,\bullet\,\bullet) - (\bullet\bullet) + (\bullet) - (0), \\ |\tilde{\Psi}_2\rangle &= \frac{1}{6}(\bullet\,\bullet\,\bullet\bullet) - \frac{3}{4}(\bullet\,\bullet\,\bullet) + \frac{4}{3}(\bullet\bullet) + \frac{1}{6}(\bullet\circ\circ\bullet) - \frac{3}{2}(\bullet) + \frac{4}{3}(0). \end{aligned}$$

Summing the coefficients of the nonabsorbing configurations in $|\tilde{\Psi}_j\rangle$, we find

$$\tilde{P}(0) = 1 - \frac{1}{2}\mu + \frac{3}{4}\mu^2 + \cdots , \tag{5.40}$$

and forming the sum of the product of coefficients and number of particles we find

$$\tilde{n}(0) = 2 + \frac{1}{2}\mu + \frac{1}{12}\mu^2 + \cdots . \tag{5.41}$$

**Critical Time Expansions**

The expansions in powers of $t$ are given by eq. (5.25). The terms are generated analogously to those for supercritical and subcritical expansions. The first few terms are as follows:

$$\begin{aligned} |\Psi(0)\rangle &= (\bullet\bullet), \\ S|\Psi(0)\rangle &= (\bullet\,\bullet\,\bullet) - (1+\lambda)(\bullet\bullet) + \lambda(0), \\ S^2|\Psi(0)\rangle &= (\bullet\,\bullet\,\bullet\bullet) - (3\lambda+2)(\bullet\,\bullet\,\bullet) + (1+\lambda)^2(\bullet\bullet) + 2\lambda(\bullet) - \lambda(1+\lambda)(0), \end{aligned}$$

which implies for the survival probability

$$P(t) = 1 - \lambda t + \frac{\lambda(\lambda - 1)}{2!} t^2 + \cdots, \tag{5.42}$$

and for the mean number of particles

$$n(t) = 2 + (1 - 2\lambda)t + \frac{\lambda(2\lambda - 3)}{2!} t^2 + \cdots. \tag{5.43}$$

By expanding only a few terms we realize that the higher the order we compute, the more complicated it becomes. We also notice that these terms can be easily generated by a computer algorithm. In the next section we briefly discuss how to implement this code.

## 5.6 Computer Algorithm

In this section we show how we construct an algorithm for computing the series coefficients for the ultimate survival probability in the supercritical expansion. A full listing of the program can be found in the Appendix. As we have seen, in the supercritical expansion, the term $|\psi_j\rangle$ in the probability distribution is generated according to the following recursive relation:

$$|\psi_j\rangle = (s - V)^{-1} W |\psi_{j-1}\rangle \quad j \geq 1. \tag{5.44}$$

Each configuration is represented by an odd binary integer, associating 0's with vacancies and 1's with particles. Due to translational invariance we can always represent the first occupied site (counting from right to left) as the first bit (explaining why we only consider odd numbers). Thus the configuration ($\bullet \circ \circ \bullet \bullet$) corresponds to 10011, or 19 in base ten. Let $|\psi_j\rangle = [\sum_{\mathrm{I}}$ (I) COEF[I]], where COEF[I] denotes the coefficient of configuration (I); let FILTER[K] represent two particles sitting at $k$ and $k+1$ (FILTER[K] $= 3 \cdot 2^k$) and NFILTER[K] = NOT(FILTER[K]) is the bitwise complement of FILTER[K]. According to eq. (5.22) applying $W$ to a configuration (I) containing $r$ pairs means to generate $r$ new configurations (I′) each having one of the $r$ pairs vacated. In the code, annihilation of the pair situated at $(k, k+1)$ is effected by the operation I′ = (I AND NFILTER[K]), where AND is the bitwise logical operator "AND". So, for each configuration we first search for pairs (I AND FILTER[K] = FILTER[K]) and then we annihilate them. Each new configuration takes the same coefficient as the configuration (I) it was derived from. And finally we add $-r$ times the coefficient of the original configuration (I) to the running sum for $W|\psi_j\rangle$.

Application of $(s-V)^{-1}$ is slightly more complicated due to the recursive scheme. The operation on a configuration (I) gives

$$(s-V)^{-1}(i) = (s+\sum_{k=1}^{q} f_k)^{-1}[(i) + (s-V)^{-1}\sum_{k=1}^{q} f_k(i')_k],$$

which involves (I) itself again, plus $q$ new configurations (I'), each having one additional particle, multiplied by the factor $(\sum_{k=1}^{q} f_k)^{-1}$. $q$ is the number of vacant sites that are nearest neighbors of at least one pair, and $f_k$ equals 1/2 (1) if site $k$ has one or (two) nearest-neighbor pairs. Let ">>" be the bitwise right shift operator. The operations RIGHT = (I AND FILTER[K-2]) >> (K-2) and LEFT = (I AND FILTER[K+1]) >> K, where (I >> K-2) shifts the value of (I) right by $(k-2)$ positions, filling vacated bits with zero, are tests for counting the number of neighboring pairs of site $k$. If RIGHT= 3 it means that site $k$ has one pair on the right, similarly, if LEFT= 6 site $k$ has one pair on the left. If site $k$ is vacant, or (I AND $2^k$) = 0, the new configuration is (I')= I OR $2^k$, where OR is the bitwise logical operator "OR". Noting that any new configuration (I') > (I), we iterate the operation of $(s-V)^{-1}$ over the newly generated configurations by storing them with configurations that are still to come and by treating them in ascending order.

## 5.7 Results and Analysis

**Supercritical Expansion**

| n | coefficients |
|---|---|
| 0 | 1.0 |
| 1 | -4.0 |
| 2 | -18.5 |
| 3 | -137.375 |
| 4 | -981.191162 |
| 5 | -8716.618095 |
| 6 | -78563.635407 |

Table 5.1: Coefficients of $\lambda^n$ in the supercritical expansion for the ultimate survival probability $P_\infty$.

The coefficients of the supercritical series we derived for the ultimate survival probability are listed in Table 5.1. We are only able to generate terms to 6th order in $\lambda$. This is a consequence of limited memory: configurations with up to $(3n+1)$ particles contribute to the extinction probability at $n$-th order, requiring storage and analysis of about $2^{3n}$ integers. This gets more complicated when coupled with the iterative nature of the operator $(s-V)^{-1}$. Numerous attempts to optimize the code were made, unfortunately none of them successful.

We analyze the supercritical series for $P_\infty$ using the Padé approximants (discussed in chapter 2). In section (4.4) we found that $P_\infty \propto (\lambda - \lambda_c)^\beta$. Thus by forming the Padé approximants for the $(d/d\lambda) \ln P_\infty$ series, we obtain estimates for $\lambda_c$, which is associated with the first positive pole in the real axis. From our analysis we estimate $\lambda_c = 0.08285; 0.08255$ and $0.08334$ using the approximants [3,3], [3,2] and [2,3], respectively. We see that these values are in reasonable agreement with the simulation value $\lambda_c^s = 0.0835$ [40]. Given the small number of terms, we could not expect much closer agreement. For the exponent $\beta$, given by the residue of the Padé approximant at this pole, we did not obtain any useful estimate.

**Subcritical Expansions**

In the subcritical regime we derived series for the ultimate survival probability and the mean number of particles in terms of $\mu = \lambda^{-1}$ to $\mathrm{O}(\mu^{16})$. The coefficients of these series are listed in Table 5.2.

For the subcritical series we are able to compute a few more terms, as we only have to keep configurations with $n+3$ particles at most, for each order $n$.

In section (4.4) we saw that the survival probability can be written as

$$P(t) \sim t^{-\delta} \phi(\Delta t^{1/\nu_\parallel}). \tag{5.45}$$

In the subcritical regime, far from the critical point, it is expected that the survival probability decays exponentially, as the correlations are of short range. This can be the case only if

$$\phi(y) \sim (-y)^{\delta\nu_\parallel} \ \exp[-b(-y)^{\nu_\parallel}] \quad \text{for} \quad y \to -\infty \tag{5.46}$$

where $b$ is a constant. Substituting the above relation in the equation for $P(t)$ we find

$$P(t) \propto (-\Delta)^{\delta\nu_\parallel} \ \exp[-b(-\Delta)^{\nu_\parallel} t]. \tag{5.47}$$

| n | $\tilde{P}(0)$ | $\tilde{n}(0)$ |
|---|---|---|
| 0 | 1.0 | 2.0 |
| 1 | -0.5 | 0.5 |
| 2 | 0.75 | -0.0833332 |
| 3 | -1.04167 | 0.236111 |
| 4 | 1.47639 | -0.407871 |
| 5 | -2.10222 | 0.697969 |
| 6 | 3.00454 | -1.17181 |
| 7 | -4.31084 | 1.94812 |
| 8 | 6.2118 | -3.21551 |
| 9 | -8.99266 | 5.27555 |
| 10 | 13.0808 | -8.61069 |
| 11 | -19.1188 | 13.993 |
| 12 | 28.0753 | -22.6583 |
| 13 | -41.4156 | 36.5826 |
| 14 | 61.3616 | -58.9276 |
| 15 | -91.2924 | 94.7496 |
| 16 | 136.361 | -152.135 |

Table 5.2: Coefficients of $\mu^n$ in the subcritical expansions for the survival probability $\tilde{P}(0)$ and $\tilde{n}(0)$.

The Laplace transform of this relation yields

$$\tilde{P}(s) = \int_0^\infty P(t)e^{-st}dt \propto \frac{(-\Delta)^{\delta\nu_\parallel}}{s + b(-\Delta)^{\nu_\parallel}}. \tag{5.48}$$

By allowing $s \to 0$ and making use of the relation $\beta = \delta\nu_\parallel$, we find that

$$\tilde{P}(0) \propto (-\Delta)^{\beta-\nu_\parallel}. \tag{5.49}$$

Analogously, we expect that the mean number of particles decays exponentially in the subcritical regime. A procedure similar to the one used to get $\tilde{P}(0)$ yields

$$\tilde{n}(0) \propto (-\Delta)^{-\nu_\parallel(1+\eta)}. \tag{5.50}$$

By regarding the expressions for $\tilde{P}(0)$ and for $\tilde{n}(0)$, and forming the Padé approximants for $(d/d\mu)\ln\tilde{P}(0)$ and $(d/d\mu)\ln\tilde{n}(0)$ we find the following estimates for $\mu_c$:

$[8,8] = 12.96092$ and $[8,8] = 10.6425$, respectively. These values should be compared to the simulation value $\mu_c^s = 11.9702$.

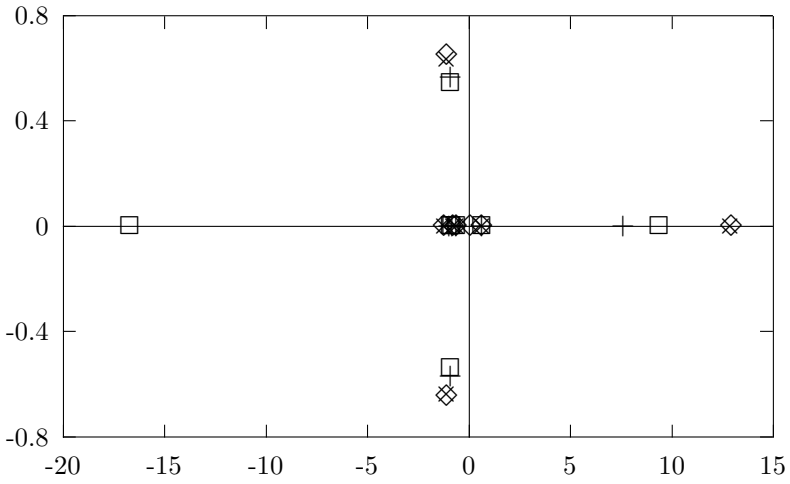


Figure 5.3: Plot in the complex-$\mu$ plane of the poles of the following Padé approximants: [8,8] $\diamond$; [8,7] $+$; [7,8] $\Box$; and [7,7] $\times$; for $(d/d\mu)\ln\tilde{P}(0)$.

Although we have generated a significantly larger number of terms for the subcritical expansions, compared to the supercritical case, we notice that the estimates for $\mu_c$ are quite poor. In fact, the alternating sign of the coefficients is a clue that the dominant singularity might lie on the negative real axis. The off-diagonal Padé approximants yield even worse estimates. In Fig. (5.3) we plot a few of the typical sets of poles. This plot confirms that the dominant singularity lies on the negative real axis, and that several poles lie nearer the origin than the physical singularity. The latter circumstance renders extraction of useful estimates very difficult.

**Critical Time Expansions**

From section (5.5), we see that the series for $P(t)$ and $n(t)$ in powers of $t$ are given by

$$\begin{aligned} P(t,\lambda) &= 1 - \lambda t + \cdots, \\ n(t,\lambda) &= 2 + (1-2\lambda)t + \cdots. \end{aligned}$$

As the asymptotic evolution of the survival probability and the mean number of particles in the critical process are governed by power laws: $P(t;\lambda_c) \propto t^{-\delta}, n(t;\lambda_c) \propto$

$t^\eta$, our goal is to study these series for $\lambda = \lambda_c$ and try to obtain estimates for the exponents $\delta$ and $\eta$. In Table 5.3 we show the coefficients for the power-$t$ series of $P(t)$ and $n(t)$ calculated at $\lambda_c^s = 0.0835$.

| n | $P(t)$ | $n(t)$ |
|---|---|---|
| 0 | 1.0 | 2.0 |
| 1 | -8.354101E-02 | 8.329180E-01 |
| 2 | -3.828096E-02 | -1.183324E-01 |
| 3 | 3.240256E-02 | -3.649198E-03 |
| 4 | -1.042570E-02 | 8.151837E-03 |
| 5 | 1.245138E-03 | -2.403629E-03 |
| 6 | 3.366557E-04 | 4.046221E-04 |
| 7 | -2.030486E-04 | -3.847422E-05 |
| 8 | 5.147464E-05 | -2.286139E-06 |
| 9 | -7.647985E-06 | 2.537779E-06 |
| 10 | 4.932625E-07 | -8.720479E-07 |
| 11 | 5.824816E-08 | 2.071887E-07 |
| 12 | -1.688591E-08 | -3.647137E-08 |
| 13 | 1.826442E-09 | 1.498052E-08 |
| 14 | 3.396279E-08 | -2.434431E-08 |
| 15 | -8.479775E-08 | -5.103685E-09 |
| 16 | 1.367656E-07 | 8.715569E-08 |
| 17 | -1.508317E-06 | 2.156652E-06 |

Table 5.3: Series coefficients for the survival probability $P(t)$ and the mean number of particles $n(t)$.

Following the method applied in [30], we transform these series using

$$F[f(t)] = t\frac{d\ln f(t)}{dt} \tag{5.51}$$

where $f(t)$ is the Taylor series expansion of some quantity about $t = 0$. If $f(t) \sim At^\alpha$, its transform remains finite in the limit $t \to \infty$, as $F(t) \to \alpha$, and also provides information about the exponents.

We study the long-time behavior of $F[P(t)]$ and $F[n(t)]$ via the diagonal Padé approximants, as the off-diagonal approximants have trivial $t \to \infty$ limits. Unfortunately, this series does not provide any reasonable estimates of the exponents $\delta$ and

$\eta$. For example, the estimates yielded by the [8,8] and [7,7] approximants for the exponent $\delta$ are: 4.591 and 6.051. From simulations we know that $\delta^s = 0.250(5)$ [40]. The irregular patterns of the signs and magnitudes of the terms in these expansions are indicative of poorly-behaved series.

It is important to remark that all actual calculations are done with $s = 0$.

# Chapter 6

# Conclusions and Outlook

We studied the diluted contact process through mean-field cluster expansions. Our results identify a continuous absorbing-state transition located at the critical value of the creation parameter $\lambda_c(x)$, which depends on the dilution $x$. The dependence of the critical parameter on the dilution is approximately described by the relation $\lambda_c(x) \approx \lambda_c(0)/(1-x)$, as long as $x << 1 - p_c$. In agreement with purely heuristic arguments we thus verify that the reduction of effective neighbors caused by dilution is compensated by an increase in the critical creation parameter.

Our numerical simulations for dilutions $x \geq 0.05$ indicate that the critical behavior of the diluted contact process is markedly different from that of the pure contact process, as expected on the basis of the Harris criterion [44]. We found that, unlike the pure case in which all three quantities behave as power-laws, the survival probability and the mean-square spreading of particles exhibit a logarithmic asymptotic dependence on time and the population size goes to a constant. These results show how the presence of disorder impairs the ability of the critical process to survive and expand [67].

We also applied time-dependent series expansions to the pair-contact process in the critical and off-critical regimes. Despite the limited number of terms available, the supercritical expansions yielded a reasonable location of the critical point. On the other hand, the subcritical expansions yield poorer results despite the availability of more terms. This is because the dominant negative singularity is closer to the origin than the physical singularity is, preventing us from getting good estimates of the critical parameter. Our next step regarding the subcritical and also the critical time series is to find an appropriate transformation in order to remove the dominant singularity from the vicinity of the origin. Finally there is also the possibility of

generating more terms for these series. Such an approach involves no conceptual difficulties, but can only be pursued with the use of more efficient machines.

# Appendix

**Program to calculate supercritical expansion of the ultimate survival probability for the one-dimensional pair-contact process.**
(Programming language: C)

```
# include <stdio.h>
# include <math.h>
C Definition of constants
# define N 6
# define Nm (3*N+1)
# define q 524288
FILE *fp;
C Global variables
double coef[q];
long int v[Nm],filter[Nm],nfilter[Nm];
int bits[q];
C Subroutine for the operation (s − V)^{-1}
void create() {
long int k,a,b,d,e,f,i,j,lm,test,LP,RP;
double sum,ncoef[q],aux[q],aux1;
extern double coef[q];
extern long int v[Nm];
char stop;
C Initialization of local variables
ncoef[0] = 0;
for(j=1;j<q;j+=2) ncoef[j] = 0;
C Loop for each configuration k
for(k=1;k<q;k+=2)
if (coef[k]!=0) {
```

```
SUM = 0.0;
AUX1 = COEF[K]/2;
AUX[0] = 0.0;
FOR(J=1;J<Q;J+=2) AUX[J] = 0.0;
C Locating the leftmost occupied site
LM = BITS[K];
C Applying (s − V)^−1 to the first and the last sites
IF (LM==NM) {
IF ((K & 3) == 3) SUM = SUM + 0.5;
A = 3 * V[NM-2];
IF ((K & A) == A) SUM = SUM + 0.5; }
IF (LM<NM) {
A = K << 1;
LP = 6;
RP = 7 * V[LM-2];
B = (A & LP) >> 1;
IF (B==3) {
AUX[A+1] = AUX[A+1] + AUX1;
SUM = SUM + 0.5; }
B = (K & RP) >> (LM-2);
IF (B==3) {
F = K | V[LM];
AUX[F] = AUX[F] + AUX1;
SUM = SUM + 0.5; }
}
C Applying (s − V)^−1 to the other sites
LM−−;
FOR(J=1;J<LM;J++) {
A = K & V[J];
C Testing if site j is vacant
IF (A==0) {
LP = 3 * V[J+1];
IF (J!=1) RP = 3 * V[J-2];
D = (K & LP) >> (J+1);
IF (J!=1) E = (K & RP) >> (J-2); ELSE E = 0;
C Counting the number of neighboring pairs of site j
```

```
IF (D==3 && E==3) {
SUM = SUM + 1.;
F = K | V[J];
AUX[F] = AUX[F] + COEF[K];
}
ELSE IF (D==3 || E==3) {
SUM = SUM + 0.5;
F = K | V[J];
AUX[F] = AUX[F] + AUX1; }
}}
IF (SUM==0.0) SUM = 1.0;
FOR(J=K+2;J<Q;J+=2) COEF[J] = COEF[J] + AUX[J]/SUM;
NCOEF[K] = NCOEF[K] + COEF[K]/SUM;
}
NCOEF[0] = COEF[0];
FOR(J=1;J<Q;J+=2) COEF[J] = NCOEF[J];
}
```

**C Subroutine for the operation $W$**

```
VOID ANNIHILATE() {
LONG INT K,M,TEMP,J,NPAIR;
CHAR STOP;
DOUBLE NCOEF[Q];
EXTERN DOUBLE COEF[Q];
EXTERN LONG INT V[NM],FILTER[NM],NFILTER[NM];
```

**C Initialization of local variables**

```
NCOEF[0] = 0;
FOR(J=1;J<Q;J+=2) NCOEF[J] = 0;
```

**C Loop for each configuration k**

```
FOR(K=3;K<Q;K+=2)
IF (COEF[K]!=0) {
NPAIR = 0;
J = 0;
STOP = 0;
```

**C Counting the number of pairs of each configuration**

```
WHILE(STOP==0) {
IF (FILTER[J]>K) STOP = 1;
```

```
IF (K>=FILTER[J]) {
M = (K & FILTER[J]) >> J;
IF (M==3) {
NPAIR = NPAIR + 1;
```
**Annihilating one pair at configuration k**
```
TEMP = K & (NFILTER[J]);
IF (J==0 && TEMP!=0) WHILE((TEMP%2)==0) TEMP = TEMP >> 1;
NCOEF[TEMP] = NCOEF[TEMP] + COEF[K]; }
}
J++;
}
NCOEF[K] = NCOEF[K] - NPAIR * COEF[K];
}
COEF[0] = NCOEF[0];
FOR(J=1;J<Q;J+=2) COEF[J] = NCOEF[J];
}
```
**Main Program**
```
MAIN() {
EXTERN DOUBLE COEF[];
EXTERN LONG INT V[NM],FILTER[NM], NFILTER[NM];
EXTERN INT BITS[Q];
LONG INT Z,J,I,NPAIR,K,M;
DOUBLE PSI;
CHAR STOP;
FP = FOPEN("SUPER.DATA","W");
```
**Setting the initial state $|\chi_0\rangle$**
```
FOR(I=0;I<Q;I++) COEF[I] = 0;
COEF[3] = 1.0;
FOR(I=0;I<NM;I++) {
V[I] = POW(2,I);
FILTER[I] = 3 * V[I];
NFILTER[I] =  FILTER[I]; }
```
**Storing the number of bits of each configuration**
```
BITS[0] = 1;
BITS[1] = 1;
J = 2;
```

```
FOR(I=3;I<Q;I+=2) {
IF (I<POW(2,J)) BITS[I] = J;
IF (I>POW(2,J)) {
J++;
BITS[I] = J;
}}
```

**Generating $|\psi(0)\rangle$**

```
CREATE();
```

**Generating the other $|\psi(j)\rangle$ to $N$-th order**

```
FOR(Z=1;Z<=N;Z++) {
IF (Z==N) ANNIHILATE();
ELSE {
ANNIHILATE();
CREATE(); }
PSI = 0;
```

**Identifying the absorbing configurations**

```
FOR(K=0;K<Q;K++)
IF (COEF[K]!=0) {
NPAIR = 0;
J = 0;
STOP = 0;
WHILE(STOP==0) {
IF (FILTER[J]>K) STOP = 1;
IF (K>=FILTER[J]) {
M = (K & FILTER[J]) >> J;
IF (M==3) NPAIR = NPAIR + 1; }
IF (NPAIR>=1) STOP = 1;
J++;
}
```

**The coefficients of the absorbing configurations are stored at PSI**

```
IF (NPAIR==0) PSI = PSI - COEF[K];
}
FPRINTF(FP,"% D % F  N",Z,PSI);
}}
```

# References


[1] T. E. Harris, Ann. Prob. **2**, 969 (1974).

[2] T.M. Liggett, *Interacting Particle Systems* (Springer-Verlag, New York, 1985).

[3] G. Grinstein, Z.-W. Lai and Dana A. Browne, Phys. Rev. A **40**, 4820 (1989).

[4] H.K. Janssen, Z. Physik B **42**, 151 (1981).

[5] P. Grassberger, Z. Physik B **47**, 365 (1982).

[6] P. Grassberger, J. Stat. Phys. **79**, 13 (1995).

[7] R. Durrett, *Lecture Notes on Particle Systems and Percolation* (Wadsworth, Pacific Grove, CA, 1988).

[8] P. Grassberger, J. Phys. A **22**, 3673 (1989).

[9] M. Moshe, Phys. Rep. **33C**, 255 (1977).

[10] P. Grassberger and K. Sundermeyer, Phys. Lett. **88 B**, 220 (1978).

[11] J.L. Cardy and R.L. Sugar, J. Phys. A **13**, L423 (1980).

[12] R.M. Ziff, E. Gulari and Y. Barshad, Phys. Rev. Lett. **56**, 2553 (1986).

[13] J. Marro and R. Dickman, *Nonequilibrium Phase Transitions* (Cambridge Press, 1997), in press.

[14] R. Dickman and M. Burschka, Phys. Lett. A **127**, 132 (1988).

[15] I. Jensen, H.C. Fogedby and R. Dickman, Phys. Rev. A **41**, 3411 (1990).

[16] B. Widom, J. Chem. Phys. **43**, 3898 (1965).

[17] L.P. Kadanoff, Physics (N.Y.) **2**, 263 (1966).

[18] K.G. Wilson, Phys. Rev. B **4**, 3174 (1971).

[19] T. Aukrust, D. A. Browne, and I. Webman, Phys. Rev. A **41**, 5294 (1990).

[20] M.E. Fisher, in *Proceedings of the Enrico Fermi International School of Physics*, Vol. 51, edited by M.S. Green (Academic Press, Varenna, Italy, 1971). M.E. Fisher and M.N. Barber, Phys. Rev. Lett. **28**, 1516 (1972).

[21] M.N. Barber, in *Phase Transitions and Critical Phenomena*, Vol. 8, edited by C. Domb and J.L. Lebowitz, (Academic Press, New York, 1983).

[22] P. Grassberger and A. de la Torre, Ann. Phys. (N. Y.) **122**, 373 (1979).

[23] D. ben-Avraham and J. Köhler, Phys. Rev. A **45**, 8358 (1992).

[24] M.C. Marques, Physica A **163**, 915 (1990).

[25] M.C. Marques, J. Phys. A **23**, 3389 (1990).

[26] M. Droz, L. Frachebourg and M.C. Marques, J. Phys. A **24**, 2869 (1991).

[27] R. Dickman, J. Stat. Phys. **55**, 997 (1989).

[28] W. Kinzel, Z. Phys. B **58**, 229 (1985).

[29] R. Dickman and I. Jensen, Phys. Rev. Lett. **67**, 2391 (1991).

[30] I. Jensen and R. Dickman, J. Stat. Phys. **71**, 89 (1993).

[31] A.J. Guttmann, *Phase Transitions and Critical Phenomena*, Vol. 13, edited by C. Domb and J. Lebowitz (Academic Press, New York, 1989).

[32] G.A. Baker Jr.,*Quantitative Theory of Critical Phenomena* (Academic Press, New York, 1990).

[33] G.A. Baker Jr.,*Essentials of Padé Approximants* (Academic Press, New York, 1975).

[34] I. Jensen, *Computer Simulations and Analytical Studies of Non-equilibrium Phase Transitions in Interacting Particle Systems with Absorbing States* (Ph.-D. Thesis, Århus, Denmark, 1992).

[35] B. Chopard and M. Droz, J. Phys. A **21**, 205 (1988).

[36] J. Mai and W. van Niessen, Phys. Rev. A **44**, 6165 (1991).

[37] K.G. Wilson and J. Kogut, Phys. Rep. **12C**, 75 (1974).

[38] I. Jensen, J. Phys. A **27**, L61 (1994).

[39] I. Jensen, Phys. Rev. Lett. **70**, 1465 (1993).

[40] I. Jensen and R. Dickman, Phys. Rev. E **48**, 1710 (1993).

[41] R. Dickman,"Critical Phenomena at Absorbing States," Ch. 3 of *Nonequilibrium Statistical Mechanics in One Dimension*, V. Privman, Ed. (Cambridge Press, 1996).

[42] I. Jensen, Phys. Rev. E **47**, 1 (1993).

[43] I. Jensen, Phys. Rev. E **50**, 3623 (1994).

[44] A. B. Harris, J. Phys. **C 7**, 1671 (1974).

[45] T.C. Lubensky, *Critical Phenomena in Random Systems* (North-Holland Publishing Company, 1979).

[46] R.J. Birgeneau, R.A. Cowley, G. Shirane and H.J. Guggenheim, Phys. Rev. Lett. **37**, 940 (1973).

[47] R. Malmhall, K.V. Rao, G. Backstrom and S.M. Bhagat, Physica **86-88D**, 196 (1977).

[48] See R.B. Stinchcombe, *Phase Transitions*, v. 7, C. domb and J.L. Lebowitz, eds., (Academic Press London, 1983).

[49] S. Ma, *Modern Theory of Critical Phenomena* (W.A Benjamin Inc. Massachussetts, 1976).

[50] D. Andelman and A.N. Berker, Phys. Rev. **29**, 2630 (1984).

[51] A. N. Berker, Physica A **194**, 72 (1993).

[52] R. Schinazi, "Uma Introdução aos Processos Estocásticos Espaciais" (20 Colóquio Brasileiro de Matemática - IMPA - RJ, 1995).

[53] C. Bezuidenhout and G. Grimmett, Ann. Prob. **18**, 1462 (1990).

[54] R.C. Brower, M.A. Furman and M. Moshe, Phys. Lett. B **76**, 213 (1978).

[55] J.F.F. Mendes, R. Dickman, M. Henkel and M.C. Marques, J. Phys. A **27**, 3019 (1994).

[56] A.J. Noest, Phys. Rev. B **38**, 2715 (1988).

[57] A. J. Noest, Phys. Rev. Lett. **57**, 90 (1986).

[58] P. Grassberger, private communication.

[59] R.B. Griffiths, Phys. Rev. Lett. **23**, 17 (1969)

[60] S. P. Obukhov, JEPT Lett. **45**, 172 (1987).

[61] M. Bramson, R. Durrett, and R.H. Schonmann, Ann. Prob. **19** 960, (1991).

[62] D. ben-Avraham, I. Webman, and I. Kanter, in preparation.

[63] L. Peliti, J. Physique **46**, 1469 (1985).

[64] P. Grassberger and M. Scheunert, Fortschritte der Physik **28**, 547 (1980).

[65] M. Doi, J. Phys. A **9**, 1479 (1976).

[66] R. Dickman, Phys. Rev. **E53**, 2223 (1996).

[67] A.G. Moreira and R. Dickman, Phys. Rev. E **54**, 3090 (1996).